22. **Kitada T,** Asakawa S, Hattori N, *et al*. Mutations in the parkin gene cause autosomal recessive juvenile parkinsonism. *Nature* 1998;**392**:605—8.
23. **Hattori N,** Kitada T, Matsumine H, *et al*. Molecular genetic analysis of a novel parkin gene in Japanese families with autosomal recessive juvenile parkinsonism: evidence for variable homozygous deletions in the parkin gene in affected individuals. *Ann Neurol* 1998;**44**:935—41.
24. **Matsumine H,** Saito M, Shimoda-Matsubayashi S, *et al*. Localization of a gene for an autosomal recessive form of juvenile Parkinsonism to chromosome 6q25.2-27. *Am J Hum Genet* 1997;**60**:588—96.
25. **Mori H,** Kondo T, Yokochi M, *et al*. Pathologic and biochemical studies of juvenile parkinsonism linked to chromosome 6q. *Neurology* 1998;**51**:890—2.
26. **Takahashi H,** Ohama E, Suzuki S, *et al*. Familial juvenile parkinsonism: clinical and pathologic study in a family. *Neurology* 1994;**44**:437—41.
27. **Farrer M,** Chan P, Chen R, *et al*. Lewy bodies and parkinsonism in families with parkin mutations. *Ann Neurol* 2001;**50**:293—300.
28. **Hilker R,** Klein C, Ghaemi M, *et al*. Positron emission tomographic analysis of the nigrostriatal dopaminergic system in familial parkinsonism associated with mutations in the parkin gene. *Ann Neurol* 2001;**49**:367—76.
29. **Khan NL,** Brooks DJ, Pavese N, *et al*. Progression of nigrostriatal dysfunction in a parkin kindred: an [18F]dopa PET and clinical study. *Brain* 2002;**125**:2248—56.
30. **Klein C,** Pramstaller PP, Kis B, *et al*. Parkin deletions in a family with adult-onset, tremor-dominant parkinsonism: expanding the phenotype. *Ann Neurol* 2000;**48**:65—71.
31. **Pramstaller PP,** Kis B, Eskelson C, *et al*. Phenotypic variability in a large kindred (Family LA) with deletions in the parkin gene. *Mov Disord* 2002;**17**:424—6.
32. **Lincoln SJ,** Maraganore DM, Lesnick TG, *et al*. Parkin variants in North American Parkinson's disease: cases and controls. *Mov Disord* 2003;**18**:1306—11.
33. **Kay DM,** Moran D, Moses L, *et al*. Heterozygous parkin point mutations are as common in control subjects as in Parkinson's patients. *Ann Neurol* 2007;**61**:47—54.
34. **Shimura H,** Hattori N, Kubo S, *et al*. Familial Parkinson disease gene product, parkin, is a ubiquitin-protein ligase. *Nat Genet* 2000;**25**:302—5.
35. **Matsuda N,** Kitami T, Suzuki T, *et al*. Diverse effects of pathogenic mutations of Parkin that catalyze multiple monoubiquitylation in vitro. *J Biol Chem* 2006;**281**:3204—9.
36. **Shimura H,** Schlossmacher MG, Hattori N, *et al*. Ubiquitination of a new form of alpha-synuclein by parkin from human brain: implications for Parkinson's disease. *Science* 2001;**293**:263—9.
37. **Chung KK,** Zhang Y, Lim KL, *et al*. Parkin ubiquitinates the alpha-synuclein-interacting protein, synphilin-1: implications for Lewy-body formation in Parkinson disease. *Nat Med* 2001;**7**:1144—50.
38. **Weihofen A,** Thomas KJ, Ostaszewski BL, *et al*. Pink1 forms a multiprotein complex with Miro and Milton, linking Pink1 function to mitochondrial trafficking (dagger). *Biochemistry* 2009;**48**:2045—52.
39. **Narendra D,** Tanaka A, Suen DF, *et al*. Parkin is recruited selectively to impaired mitochondria and promotes their autophagy. *J Cell Biol* 2008;**183**:795—803.
40. **Narendra D,** Kane LA, Hauser DN, *et al*. p62/SQSTM1 is required for Parkin-induced mitochondrial clustering but not mitophagy; VDAC1 is dispensable for both. *Autophagy* 2010;**6**:1090—106.
41. **Matsuda N,** Sato S, Shiba K, *et al*. PINK1 stabilized by mitochondrial depolarization recruits Parkin to damaged mitochondria and activates latent Parkin for mitophagy. *J Cell Biol* 2010;**189**:211—21.
42. **Park J,** Lee G, Chung J. The PINK1—Parkin pathway is involved in the regulation of mitochondrial remodeling process. *Biochem Biophys Res Commun* 2009;**378**:518—23.
43. **Valente EM,** Bentivoglio AR, Dixon PH, *et al*. Localization of a novel locus for autosomal recessive early-onset parkinsonism, PARK6, on human chromosome 1p35-p36. *Am J Hum Genet* 2001;**68**:895—900.
44. **Valente EM,** Abou-Sleiman PM, Caputo V, *et al*. Hereditary early-onset Parkinson's disease caused by mutations in PINK1. *Science* 2004;**304**:1158—60.
45. **Marongiu R,** Brancati F, Antonini A, *et al*. Whole gene deletion and splicing mutations expand the PINK1 genotypic spectrum. *Hum Mutat* 2007;**28**:98.
46. **Hatano Y,** Li Y, Sato K, *et al*. Novel PINK1 mutations in early-onset parkinsonism. *Ann Neurol* 2004;**56**:424—7.
47. **Samaranch L,** Lorenzo-Betancor O, Arbelo JM, *et al*. PINK1-linked parkinsonism is associated with Lewy body pathology. *Brain* 2010;**133**:1128—42.
48. **Kawajiri S,** Saiki S, Sato S, *et al*. Genetic mutations and functions of PINK1. *Trends Pharmacol Sci* 2011;**32**:573—80.
49. **Beilina A,** Van Der Brug M, Ahmad R, *et al*. Mutations in PTEN-induced putative kinase 1 associated with recessive parkinsonism have differential effects on protein stability. *Proc Natl Acad Sci U S A* 2005;**102**:5703—8.
50. **Pridgeon JW,** Olzmann JA, Chin LS, *et al*. PINK1 protects against oxidative stress by phosphorylating mitochondrial chaperone TRAP1. *PLoS Biol* 2007;**5**:e172.
51. **Silvestri L,** Caputo V, Bellacchio E, *et al*. Mitochondrial import and enzymatic activity of PINK1 mutants associated to recessive parkinsonism. *Hum Mol Genet* 2005;**14**:3477—92.
52. **Sim CH,** Lio DS, Mok SS, *et al*. C-terminal truncation and Parkinson's disease-associated mutations down-regulate the protein serine/threonine kinase activity of PTEN-induced kinase-1. *Hum Mol Genet* 2006;**15**:3251—62.
53. **Murata H,** Sakaguchi M, Jin Y, *et al*. A new cytosolic pathway from a Parkinson disease-associated kinase, BRPK/PINK1: activation of AKT via mTORC2. *J Biol Chem* 2011;**286**:7182—9.
54. **Plun-Favreau H,** Klupsch K, Moisoi N, *et al*. The mitochondrial protease HtrA2 is regulated by Parkinson's disease-associated kinase PINK1. *Nat Cell Biol* 2007;**9**:1243—52.
55. **Strauss KM,** Martins LM, Plun-Favreau H, *et al*. Loss of function mutations in the gene encoding Omi/HtrA2 in Parkinson's disease. *Hum Mol Genet* 2005;**14**:2099—111.
56. **Wang X,** Schwarz TL. The mechanism of Ca2+ -dependent regulation of kinesin-mediated mitochondrial motility. *Cell* 2009;**136**:163—74.
57. **Liu W,** Vives-Bauza C, Acin-Perez R, *et al*. PINK1 defect causes mitochondrial dysfunction, proteasomal deficit and alpha-synuclein aggregation in cell culture models of Parkinson's disease. *PLoS One* 2009;**4**:e4597.
58. **Amo T,** Sato S, Saiki S, *et al*. Mitochondrial membrane potential decrease caused by loss of PINK1 is not due to proton leak, but to respiratory chain defects. *Neurobiol Dis* 2011;**41**:111—8.
59. **Deng H,** Dodson MW, Huang H, *et al*. The Parkinson's disease genes pink1 and parkin promote mitochondrial fission and/or inhibit fusion in Drosophila. *Proc Natl Acad Sci U S A* 2008;**105**:14503—8.
60. **Poole AC,** Thomas RE, Andrews LA, *et al*. The PINK1/Parkin pathway regulates mitochondrial morphology. *Proc Natl Acad Sci U S A* 2008;**105**:1638—43.
61. **Haque ME,** Thomas KJ, D'Souza C, *et al*. Cytoplasmic Pink1 activity protects neurons from dopaminergic neurotoxin MPTP. *Proc Natl Acad Sci U S A* 2008;**105**:1716—21.
62. **Clark IE,** Dodson MW, Jiang C, *et al*. Drosophila pink1 is required for mitochondrial function and interacts genetically with parkin. *Nature* 2006;**441**:1162—6.
63. **Park J,** Lee SB, Lee S, *et al*. Mitochondrial dysfunction in Drosophila PINK1 mutants is complemented by parkin. *Nature* 2006;**441**:1157—61.
64. **Yang Y,** Gehrke S, Imai Y, *et al*. Mitochondrial pathology and muscle and dopaminergic neuron degeneration caused by inactivation of Drosophila Pink1 is rescued by Parkin. *Proc Natl Acad Sci U S A* 2006;**103**:10793—8.
65. **Kawajiri S,** Saiki S, Sato S, *et al*. PINK1 is recruited to mitochondria with parkin and associates with LC3 in mitophagy. *FEBS Lett* 2010;**584**:1073—9.
66. **Youle RJ,** Narendra DP. Mechanisms of mitophagy. *Nat Rev Mol Cell Biol* 2011;**12**:9—14.
67. **Abou-Sleiman PM,** Healy DG, Quinn N, *et al*. The role of pathogenic DJ-1 mutations in Parkinson's disease. *Ann Neurol* 2003;**54**:283—6.
68. **Bandopadhyay R,** Kingsbury AE, Cookson MR, *et al*. The expression of DJ-1 (PARK7) in normal human CNS and idiopathic Parkinson's disease. *Brain* 2004;**127**:420—30.
69. **Neumann M,** Muller V, Gorner K, *et al*. Pathological properties of the Parkinson's disease-associated protein DJ-1 in alpha-synucleinopathies and tauopathies: relevance for multiple system atrophy and Pick's disease. *Acta Neuropathol* 2004;**107**:489—96.
70. **Olzmann JA,** Bordelon JR, Muly EC, *et al*. Selective enrichment of DJ-1 protein in primate striatal neuronal processes: implications for Parkinson's disease. *J Comp Neurol* 2007;**500**:585—99.
71. **Usami Y,** Hatano T, Imai S, *et al*. DJ-1 associates with synaptic membranes. *Neurobiol Dis* 2011;**43**:651—62.
72. **Miller DW,** Ahmad R, Hague S, *et al*. L166P mutant DJ-1, causative for recessive Parkinson's disease, is degraded through the ubiquitin-proteasome system. *J Biol Chem* 2003;**278**:36588—95.
73. **Goldberg MS,** Pisani A, Haburcak M, *et al*. Nigrostriatal dopaminergic deficits and hypokinesia caused by inactivation of the familial parkinsonism-linked gene DJ-1. *Neuron* 2005;**45**:489—96.
74. **Wang Z,** Liu J, Chen S, *et al*. DJ-1 modulates the expression of Cu/Zn-superoxide dismutase-1 through the Erk1/2-Elk1 pathway in neuroprotection. *Ann Neurol* 2011;**70**:591—9.
75. **Lev N,** Roncevic D, Ickowicz D, *et al*. Role of DJ-1 in Parkinson's disease. *J Mol Neurosci* 2006;**29**:215—25.
76. **Fu K,** Ren H, Wang Y, *et al*. DJ-1 inhibits TRAIL-induced apoptosis by blocking pro-caspase-8 recruitment to FADD. *Oncogene*. Published Online First: 25 July 2011. doi:10.1038/onc.2011.315.
77. **Xiong H,** Wang D, Chen L, *et al*. Parkin, PINK1, and DJ-1 form a ubiquitin E3 ligase complex promoting unfolded protein degradation. *J Clin Invest* 2009;**119**:650—60.
78. **Paisan-Ruiz C,** Jain S, Evans EW, *et al*. Cloning of the gene containing mutations that cause PARK8-linked Parkinson's disease. *Neuron* 2004;**44**:595—600.
79. **Zimprich A,** Biskup S, Leitner P, *et al*. Mutations in LRRK2 cause autosomal-dominant parkinsonism with pleomorphic pathology. *Neuron* 2004;**44**:601—7.
80. **Berwick DC,** Harvey K. LRRK2 signaling pathways: the key to unlocking neurodegeneration? *Trends Cell Biol* 2011;**21**:257—65.
81. **Cookson MR.** The role of leucine-rich repeat kinase 2 (LRRK2) in Parkinson's disease. *Nat Rev Neurosci* 2010;**11**:791—7.
82. **Gilks WP,** Abou-Sleiman PM, Gandhi S, *et al*. A common LRRK2 mutation in idiopathic Parkinson's disease. *Lancet* 2005;**365**:415—16.
83. **Wszolek ZK,** Pfeiffer RF, Tsuboi Y, *et al*. Autosomal dominant parkinsonism associated with variable synuclein and tau pathology. *Neurology* 2004;**62**:1619—22.
84. **Ross OA,** Toft M, Whittle AJ, *et al*. Lrrk2 and Lewy body disease. *Ann Neurol* 2006;**59**:388—93.
85. **Dachsel JC,** Ross OA, Mata IF, *et al*. Lrrk2 G2019S substitution in frontotemporal lobar degeneration with ubiquitin-immunoreactive neuronal inclusions. *Acta Neuropathol* 2007;**113**:601—6.

86. **Galter D,** Westerlund M, Carmine A, *et al*. LRRK2 expression linked to dopamine-innervated areas. *Ann Neurol* 2006;**59**:714–19.
87. **Hatano T,** Kubo S, Imai S, *et al*. Leucine-rich repeat kinase 2 associates with lipid rafts. *Hum Mol Genet* 2007;**16**:678–90.
88. **Biskup S,** Moore DJ, Celsi F, *et al*. Localization of LRRK2 to membranous and vesicular structures in mammalian brain. *Ann Neurol* 2006;**60**:557–69.
89. **Smith WW,** Pei Z, Jiang H, *et al*. Leucine-rich repeat kinase 2 (LRRK2) interacts with parkin, and mutant LRRK2 induces neuronal degeneration. *Proc Natl Acad Sci U S A* 2005;**102**:18676–81.
90. **Ng CH,** Mok SZ, Koh C, *et al*. Parkin protects against LRRK2 G2019S mutant-induced dopaminergic neurodegeneration in Drosophila. *J Neurosci* 2009;**29**:11257–62.
91. **Venderova K,** Kabbach G, Abdel-Messih E, *et al*. Leucine-rich repeat kinase 2 interacts with parkin, DJ-1 and PINK-1 in a Drosophila melanogaster model of Parkinson's disease. *Hum Mol Genet* 2009;**18**:4390–404.
92. **Chan D,** Citro A, Cordy JM, *et al*. Rac1 protein rescues neurite retraction caused by G2019S leucine-rich repeat kinase 2 (LRRK2). *J Biol Chem* 2011;**286**:16140–9.
93. **Angeles DC,** Gan BH, Onstead L, *et al*. Mutations in LRRK2 increase phosphorylation of peroxiredoxin 3 exacerbating oxidative stress-induced neuronal death. *Hum Mutat* 2011;**32**:1390–7.
94. **Dusonchet J,** Kochubey O, Stafa K, *et al*. A rat model of progressive nigral neurodegeneration induced by the Parkinson's disease-associated G2019S mutation in LRRK2. *J Neurosci* 2011;**31**:907–12.
95. **Li X,** Wang QJ, Pan N, *et al*. Phosphorylation-dependent 14-3-3 binding to LRRK2 is impaired by common mutations of familial Parkinson's disease. *PLoS One* 2011;**6**: e17153.
96. **Najim al-Din AS,** Wriekat A, Mubaidin A, *et al*. Pallido-pyramidal degeneration, supranuclear upgaze paresis and dementia: Kufor-Rakeb syndrome. *Acta Neurol Scand* 1994;**89**:347–52.
97. **Ramirez A,** Heimbach A, Grundemann J, *et al*. Hereditary parkinsonism with dementia is caused by mutations in ATP13A2, encoding a lysosomal type 5 P-type ATPase. *Nat Genet* 2006;**38**:1184–91.
98. **Gitler AD,** Chesi A, Geddie ML, *et al*. Alpha-synuclein is part of a diverse and highly conserved interaction network that includes PARK9 and manganese toxicity. *Nat Genet* 2009;**41**:308–15.
99. **Ugolino J,** Fang S, Kubisch C, *et al*. Mutant Atp13a2 proteins involved in parkinsonism are degraded by ER-associated degradation and sensitize cells to ER-stress induced cell death. *Hum Mol Genet* 2011;**20**:3565–77.
100. **Tan J,** Zhang T, Jiang L, *et al*. Regulation of intracellular manganese hemeostasis by kufor-rakeb syndrome associated ATP13A2. *J Biol Chem* 2011;**286**:29654–62.
101. **Kawamoto Y,** Kobayashi Y, Suzuki Y, *et al*. Accumulation of HtrA2/Omi in neuronal and glial inclusions in brains with alpha-synucleinopathies. *J Neuropathol Exp Neurol* 2008;**67**:984–93.
102. **Kruger R,** Sharma M, Riess O, *et al*. A large-scale genetic association study to evaluate the contribution of Omi/HtrA2 (PARK13) to Parkinson's disease. *Neurobiol Aging* 2011;**32**:548 e9–18.
103. **Suzuki Y,** Takahashi-Niki K, Akagi T, *et al*. Mitochondrial protease Omi/HtrA2 enhances caspase activation through multiple pathways. *Cell Death Differ* 2004;**11**:208–16.
104. **Martins LM.** The serine protease Omi/HtrA2: a second mammalian protein with a reaper-like function. *Cell Death Differ* 2002;**9**:699–701.
105. **Martins LM,** Morrison A, Klupsch K, *et al*. Neuroprotective role of the reaper-related serine protease HtrA2/Omi revealed by targeted deletion in mice. *Mol Cell Biol* 2004;**24**:9848–62.
106. **Li B,** Hu Q, Wang H, *et al*. Omi/HtrA2 is a positive regulator of autophagy that facilitates the degradation of mutant proteins involved in neurodegenerative diseases. *Cell Death Differ* 2010;**17**:1773–84.
107. **Morgan NV,** Westaway SK, Morton JE, *et al*. PLA2G6, encoding a phospholipase A2, is mutated in neurodegenerative disorders with high brain iron. *Nat Genet* 2006;**38**:752–4.
108. **Paisan-Ruiz C,** Bhatia KP, Li A, *et al*. Characterization of PLA2G6 as a locus for dystonia-parkinsonism. *Ann Neurol* 2009;**65**:19–23.
109. **Yoshino H,** Tomiyama H, Tachibana N, *et al*. Phenotypic spectrum of patients with PLA2G6 mutation and PARK14-linked parkinsonism. *Neurology* 2010;**75**:1356–61.
110. **Jenkins CM,** Wolf MJ, Mancuso DJ, *et al*. Identification of the calmodulin-binding domain of recombinant calcium-independent phospholipase A2beta. Implications for structure and function. *J Biol Chem* 2001;**276**:7129–35.
111. **Wang Z,** Ramanadham S, Ma ZA, *et al*. Group VIA phospholipase A2 forms a signaling complex with the calcium/calmodulin-dependent protein kinase IIbeta expressed in pancreatic islet beta-cells. *J Biol Chem* 2005;**280**:6840–9.
112. **Shojaee S,** Sina F, Banihosseini SS, *et al*. Genome-wide linkage analysis of a Parkinsonian-pyramidal syndrome pedigree by 500 K SNP arrays. *Am J Hum Genet* 2008;**82**:1375–84.
113. **Di Fonzo A,** Dekker MC, Montagna P, *et al*. FBXO7 mutations cause autosomal recessive, early-onset parkinsonian-pyramidal syndrome. *Neurology* 2009;**72**:240–5.
114. **Pankratz N,** Wilk JB, Latourelle JC, *et al*. Genomewide association study for susceptibility genes contributing to familial Parkinson disease. *Hum Genet* 2009;**124**:593–605.
115. **Edwards TL,** Scott WK, Almonte C, *et al*. Genome-wide association study confirms SNPs in SNCA and the MAPT region as common risk factors for Parkinson disease. *Ann Hum Genet* 2010;**74**:97–109.
116. **Hamza TH,** Zabetian CP, Tenesa A, *et al*. Common genetic variation in the HLA region is associated with late-onset sporadic Parkinson's disease. *Nat Genet* 2010;**42**:781–5.
117. **Spencer CC,** Plagnol V, Strange A, *et al*. Dissection of the genetics of Parkinson's disease identifies an additional association 5' of SNCA and multiple associated haplotypes at 17q21. *Hum Mol Genet* 2010;**20**:345–53.
118. **Liu X,** Cheng R, Verbitsky M, *et al*. Genome-wide association study identifies candidate genes for Parkinson's disease in an Ashkenazi Jewish population. *BMC Med Genet* 2011;**12**:104.
119. **Do CB,** Tung JY, Dorfman E, *et al*. Web-based genome-wide association study identifies two novel Loci and a substantial genetic component for Parkinson's disease. *PLoS Genet* 2011;**7**:e1002141.
120. **Hruska KS,** Goker-Alpan O, Sidransky E. Gaucher disease and the synucleinopathies. *J Biomed Biotechnol* 2006;**2006**:78549.
121. **Sidransky E,** Nalls MA, Aasly JO, *et al*. Multicenter analysis of glucocerebrosidase mutations in Parkinson's disease. *N Engl J Med* 2009;**361**:1651–61.
122. **Aharon-Peretz J,** Rosenbaum H, Gershoni-Baruch R. Mutations in the glucocerebrosidase gene and Parkinson's disease in Ashkenazi Jews. *N Engl J Med* 2004;**351**:1972–7.
123. **Mata IF,** Samii A, Schneer SH, *et al*. Glucocerebrosidase gene mutations: a risk factor for Lewy body disorders. *Arch Neurol* 2008;**65**:379–82.
124. **De Marco EV,** Annesi G, Tarantino P, *et al*. Glucocerebrosidase gene mutations are associated with Parkinson's disease in southern Italy. *Mov Disord* 2008;**23**:460–3.
125. **Morris HR,** Lees AJ, Wood NW. Neurofibrillary tangle parkinsonian disorders—tau pathology and tau genetics. *Mov Disord* 1999;**14**:731–6.
126. **Galpern WR,** Lang AE. Interface between tauopathies and synucleinopathies: a tale of two proteins. *Ann Neurol* 2006;**59**:449–58.
127. **Tayebi N,** Walker J, Stubblefield B, *et al*. Gaucher disease with parkinsonian manifestations: does glucocerebrosidase deficiency contribute to a vulnerability to parkinsonism? *Mol Genet Metab* 2003;**79**:104–9.
128. **Goker-Alpan O,** Stubblefield BK, Giasson BI, *et al*. Glucocerebrosidase is present in alpha-synuclein inclusions in Lewy body disorders. *Acta Neuropathol* 2010;**120**:641–9.
129. **Cullen V,** Sardi SP, Ng J, *et al*. Acid beta-glucosidase mutants linked to Gaucher disease, Parkinson disease, and Lewy body dementia alter alpha-synuclein processing. *Ann Neurol* 2011;**69**:940–53.
130. **Yap TL,** Gruschus JM, Velayati A, *et al*. Alpha-synuclein interacts with glucocerebrosidase providing a molecular link between Parkinson and Gaucher diseases. *J Biol Chem* 2011;**286**:28080–8.
131. **Hardy J.** No definitive evidence for a role for the environment in the etiology of Parkinson's disease. *Mov Disord* 2006;**21**:1790–1.
132. **Deng X,** Dzamko N, Prescott A, *et al*. Characterization of a selective inhibitor of the Parkinson's disease kinase LRRK2. *Nat Chem Biol* 2011;**7**:203–5.

SAGE-Hindawi Access to Research
Parkinson's Disease
Volume 2011, Article ID 979231, 7 pages
doi:10.4061/2011/979231

Review Article

Genetic Mutations and Mitochondrial Toxins Shed New Light on the Pathogenesis of Parkinson's Disease

Shigeto Sato and Nobutaka Hattori

Department of Neurology, Juntendo University School of Medicine, Tokyo 113-8421, Japan

Correspondence should be addressed to Nobutaka Hattori, nhattori@juntendo.ac.jp

Received 11 April 2011; Revised 2 June 2011; Accepted 12 June 2011

Academic Editor: Honglei Chen

The cellular abnormalities in Parkinson's disease (PD) include mitochondrial dysfunction and oxidative damage, which are probably induced by both genetic predisposition and environmental factors. Mitochondrial dysfunction has long been implicated in the pathogenesis of PD. The recent discovery of genes associated with the etiology of familial PD has emphasized the role of mitochondrial dysfunction in PD. The discovery and increasing knowledge of the function of PINK1 and parkin, which are associated with the mitochondria, have also enhanced the understanding of cellular functions. The PINK1-parkin pathway is associated with quality control of the mitochondria, as determined in cultured cells treated with the mitochondrial uncoupler carbonyl cyanide m-chlorophenylhydrazone (CCCP), which causes mitochondrial depolarization. To date, the use of mitochondrial toxins, for example, 1-methyl-4-phynyl-tetrahydropyridine (MPTP) and CCCP, has contributed to our understanding of PD. We review how these toxins and familial PD gene products are associated with and have enhanced our understanding of the role of mitochondrial dysfunction in PD.

1. Introduction

Parkinson's disease (PD) is the most common neurodegenerative movement disorder, affecting 1% of the population above the age of 60. The classical form of the disease is characterized clinically by rigidity, resting tremor, bradykinesia, and postural instability. In addition to these four cardinal symptoms, many nonmotor symptoms frequently appear in PD, such as cognitive impairment, hallucinations, delusion, behavioral abnormalities, depression, disturbances of sleep and wakefulness, loss of smell, pain, and autonomic dysfunctions such as constipation, hypotension, urinary frequency, impotence, and sweating. The pathological hallmarks of PD are the preferential loss of dopaminergic neurons of the substantia nigra (SN) pars compacta and formation of Lewy bodies. Exposure to environmental factors inducing mitochondrial toxin like1-methyl-4-phynyl-tetrahydropyridine (MPTP) produces selective degeneration of dopaminergic neurons in SN and results in an irreversible Parkinsonism [1–3]. The active metabolite of MPTP, 1-methyl-4-phenylpyridinium ion (MPP+), is an inhibitor of complex I, and it accumulates in dopaminergic neurons because it is actively transported via dopamine transporter (DAT) [4–6]. The inhibition of the electron transport induces oxidative damage by increasing the formation of reactive oxygen species (ROS) and leads to further mitochondrial dysfunction [7]. These findings were supported by evidence of oxidative damage including an increase in lipid peroxide [8], decrease in glutathione [9], increase in hydroxynonenal-modified proteins [10], and increase in 8-hydroxy-deoxy guanine [11] in SN. ROS impair mitochondrial proteins, further aggravating mitochondrial function. Ultimate outcomes are dissipation of mitochondrial membrane potential and the release of cytochrome c into the cytoplasm and activation of the apoptotic cascade. A biochemical link between MPTP toxicity and Parkinsonism was confirmed with the finding of low levels of complex I in the SN, skeletal muscle, and platelets in patients with PD [12, 13]. In contrast, it remains unknown whether this systemic deficiency of complex I is crucially related to dopaminergic cell loss in PD. Rats administered rotenone (an inhibitor of complex I) developed neuronal degeneration and formation of synuclein-positive

inclusions; however, the degree of complex I inhibition was not severe enough to induce brain mitochondrial dysfunction [14]. Although inhibition of complex I and production of free radical result in increased oxidative stress, it remains unclear whether such dysfunction is a primary or a secondary process in the pathogenesis of the disease.

2. Involvement of Two Mitochondrial Toxic Pathways in Synuclein, DJ-1, and Parkin Mice Model

Several mutations of the synuclein gene (SNCA) at the *PARK1* locus induce autosomal dominant Parkinsonism. Three missense mutations: A53T [15], A30P [16], and E46K [17], duplications [18–21], and triplications [22, 23] of SNCA have so far been described. Triplications are associated with Parkinsonism and dementia, and the age of onset is younger than the other mutations, and the neuropathological changes are those of diffuse Lewy body disease. Regarding the pathogenesis of *PARK1*-linked PD, accumulation of normal synuclein is likely to predispose nigral neurons for protofibril formation. Toxicity associated with increased synuclein expression is an important cellular event that enhances the genetic predisposition to sporadic PD. At present, indirect evidence suggests a relationship between synuclein and oxidative stress, including protein carbonylation and lipid peroxidation. Furthermore, synuclein-deficient mice were found to have striking resistance to MPTP-induced degeneration of dopaminergic neurons, and this resistance appeared to be related to failure of the toxin itself. Interestingly, there was dissociation in the resistance between MPTP- and rotenone-induced cell vulnerability of synuclein-null dopaminergic neurons [24]. This result suggests that MPTP associates with synuclein through another pathway independent of complex I inhibition (mitochondrial dysfunction), to finally induce dopaminergic cell death. Several mutations of the DJ-1 gene at the *PARK7* locus induce autosomal recessive Parkinsonism [25]. Clinical phenotype is characterized by an onset in the midthirties, good levodopa response, and slow disease progression. Several lines of evidence suggest that it plays a role in the oxidative stress response [26, 27]. Subcellular localization studies have shown DJ-1 to be present in the cytosol, mitochondria, and nucleus [26, 28, 29]. Junn et al. [30] showed that in response to oxidative stress, some of the DJ-1 protein is translocated from its major cytosolic pool to mitochondria and nucleus. DJ-1 null mice are vulnerable to MPTP [31]. On the other hand, Thomas et al. [32] reported that the susceptibility of SN to MPTP in mice is independent of parkin activity. In short, the absence of parkin does not seem to increase the vulnerability of dopaminergic neurons to MPTP intoxication. Another study also found that oxidative stress, including MPTP, altered parkin solubility, causing parkin aggregation, thereby suggesting parkin dysfunction as a pathogenic mechanism of sporadic PD [33].

3. Functional Interplay between PINK1 and Parkin to Maintain Mitochondrial Integrity

Many mutations of the parkin gene at the *PARK2* locus induce autosomal recessive Parkinsonism [34–38]. The usual age of onset is between 20 and 40 years. Clinical features consist of dystonia and sleep benefit, which are also characteristic symptoms. Despite affected patients responding well to levodopa, they soon develop motor fluctuations. Conversely, mutations of the PINK1 (PTEN-induced kinase 1) gene at the *PARK6* locus induce autosomal recessive Parkinsonism. The age of onset is slightly delayed relative to *PARK2*, that is, from 32 to 48 years [39]. The affected patients show levodopa-responsive Parkinsonism. PINK1 contains an N-terminal mitochondrial targeting signal and a highly conserved serine/threonine kinase domain, and many missense and nonsense mutations have been reported at the kinase domain [40–44]. In particular, the identification of PINK1 mutations has strongly implicated mitochondrial dysfunction in the pathogenesis of PD [40]. The activity of PINK1 kinase is crucial for mitochondrial maintenance via TRAP phosphorylation [45]. The loss of PINK1 function results in increased vulnerability to various stresses [46–48]. Drosophila models have demonstrated that PINK1 and parkin ensure stable mitochondrial function. Parkin null mutants show severe mitochondrial pathology associated with reduced lifespan, apoptosis, and muscle degeneration [49]. While the PINK1 mutant phenotype can be rescued by parkin gene overexpression [50, 51], the converse does not occur, suggesting that parkin acts downstream of PINK1 in a common pathway to maintain mitochondrial integrity. PINK1 loss-of-function results in reduced mitochondrial membrane potential [52], and the PINK1-parkin pathway is associated with mitochondrial elimination in cultured cells treated with the mitochondrial uncoupler carbonyl cyanide m-chlorophenylhydrazone (CCCP), which causes mitochondrial depolarization [53–58]. The exact mechanism underlying CCCP-induced mitochondrial depolarization, leading to mitochondrial autophagy, has been examined in detail. At steady state, parkin is localized throughout the cytosol but not in the mitochondria. However, parkin was rapidly recruited into the mitochondria when HeLa cells were treated with CCCP [55]. Furthermore, PINK1 recruits parkin from the cytoplasm to the low-membrane potential mitochondria, resulting in the mitochondrial degradation. Interestingly, the ubiquitin-ligase activity of parkin is repressed in the cytoplasm at steadystate; however, PINK1-dependent mitochondrial localization triggered by mitochondrial depolarization liberates the potential enzymatic activity of parkin. While CCCP is well described, its mitochondrial toxic effects provide new insights on the functional interplay between PINK1 and parkin.

4. Accumulation of PINK1 in Damaged Mitochondria

PINK1 is localized in both the mitochondria [40, 59] and the cytoplasm [55, 60]. Treatment with CCCP results in gradual accumulation of PINK1 and translocation of the cytoplasmic

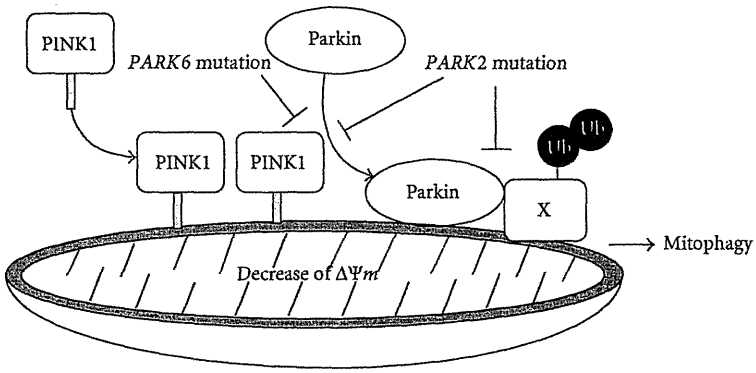

FIGURE 1: Schematic representation of PINK1-parkin-mediated mitophagy. In damaged mitochondria, PINK1 and parkin regulate mitochondrial elimination by inducing mitophagy. Under steady state, PINK1 is cleaved and degraded rapidly in the mitochondria. This process may be inhibited by the mitochondrial depolarization, resulting in PINK1 accumulation in the mitochondria. This accumulation is a crucial signal for parkin recruitment to the mitochondria. Parkin is presumed to ubiquitinate substrate (X), resulting in the induction of mitophagy.

PINK1 to the mitochondria. The subcellular localization of PINK1 is regulated by the mitochondrial membrane potential. Such accumulation may be the first trigger of PINK1-related parkin recruitment. Co-overexpression of PINK1 and parkin results in their colocalization in the mitochondria [61]. Even when these cells were not treated with CCCP, overexpression of PINK1 was associated with translocation of parkin to the cells, together with their mitochondrial aggregation.

Moreover, overexpression of both PINK1 and parkin in the cells resulted in the complete disappearance of the mitochondria. These results suggest that both PINK1 and parkin are indispensable for mitochondrial elimination and that accumulation of PINK1 in the mitochondria results in recruitment of parkin to the mitochondria even in the absence of CCCP [54].

5. PINK1 Kinase Activity Is Essential for Translocation of Parkin

PINK1 is composed of an atypical N-terminal mitochondrial targeting signal and transmembrane domain, kinase domain in the middle, and a conserved C-terminal domain, and deletion of the N-terminal amino acids abolished the mitochondrial localization of PINK1 [62]. Among other mutations, G309D, L347P, and G409V are associated with reduction in PINK1-kinase activity, and a C-terminal domain deletion mutant is associated with PINK1 dysfunction [63, 64]. The G309D/L347P/G409V mutants preserved mitochondrial localization, though their mitochondrial elimination was less compared to cells expressing both the wild-type PINK1 and parkin. When introduced into PINK1-deficient cells, the mutants were unable to complement the localization of parkin [55]. These results indicate that targeting the kinase activity and mitochondrial distribution of PINK1 is important for the mitochondrial recruitment of parkin (Figure 1).

6. PINK1 Deficiency Itself Causes Respiratory Chain Defects

Impaired mitochondrial respiration was observed in the brain of PINK1 null mice [65] although the mechanism linking PINK1 to mitochondrial membrane potential remains to be determined. Amo et al. [66] reported depletion of the mitochondrial membrane potential and cellular ATP levels (~80%) in PINK1-deficient mouse embryonic fibroblasts (MEFs) compared with those in littermate wild-type MEFs. However, loss of PINK1 did not alter mitochondrial proton leak, which reduces the membrane potential in the absence of ATP synthesis. Instead, the authors reported reduced activity of the respiratory chain, which produces the membrane potential by oxidizing substrates using oxygen. The H_2O_2 production rate by PINK1 null mitochondria was lower due to low oxygen consumption rate, while the proportion (H_2O_2 production rate per oxygen consumption rate) was higher. These results suggest that mitochondrial dysfunction in PD is not caused by proton leak, but by a defective respiratory chain. Furthermore, rate of free radical leak was significantly higher in PINK1-deficient MEFs than in wild-type MEFs. Because the differences disappeared with the addition of rotenone (inhibitor of complex I, which inhibits reverse electron flow from coenzyme Q to complex I), conceivably ROS generation enhanced by loss of PINK1 was mostly from complex I. With regard to PINK1-related PD, ROS may be an important factor. The above may also explain why cytoplasmic PINK1 protects neurons against MPTP [47]. Inhibition of complex I itself is associated with increased ROS production [67]. These results are at least in part consistent with those of previous studies, suggesting that MPTP and rotenone induce neuronal cell death by inhibiting complex I activity, leading to a PD-like phenotype [68–70] (Figure 2).

It is not doubtful that ROS generation is harmful to the cells, but the process of cell death is supposed to be slow. The crucial point is how inhibition of complex I

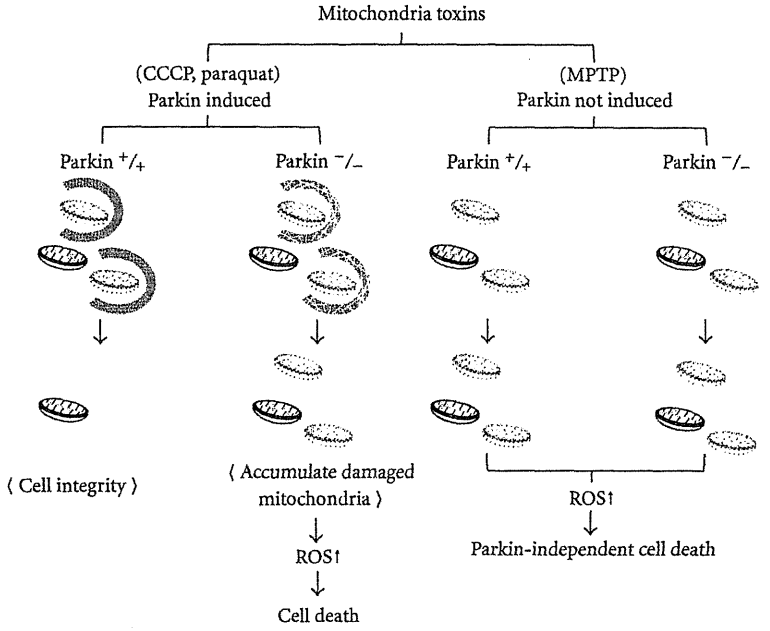

FIGURE 2: Two mechanisms of mitochondrial toxicity and parkin function. The effect of mitochondrial toxicity is different between CCCP and MPTP. Treatment with CCCP recruits parkin to the mitochondria resulting in mitophagy to keep mitochondrial integrity. Parkin deficiency is associated with accumulation of damaged mitochondria and accelerated cell death. Treatment with MPTP does not necessarily induce parkin. Parkin may be the sensor of damage-adaptive autophagy.

affects mitochondrial dysfunction including mitochondrial depolarization. Considering that the onset of *PARK6* (at 32–48 years) is slightly delayed relative to that of *PARK2* [39], some cases of PINK1 mutation might not affect parkin recruitment and thus maintain at least part of mitochondrial integrity. This may explain the late onset of *PARK6*. On the other hand, parkin did not translocate into the mitochondria when cells were treated with MPTP (our unpublished data). This finding means that inhibition of complex I does not necessarily induce low membrane potential. Further research is needed to investigate two independent pathogenic mechanisms related to MPTP and CCCP (Figure 2).

7. Conclusion

Cell death of dopaminergic neurons is due to a combination of exogenous stress and genetic predisposition. The discovery of PD genes has provided important insight including an understanding of PINK1-parkin mediated mitophagy. Furthermore, mitochondrial toxins provided crucial clues: (1) CCCP directly affects mitochondrial dysfunction and induces mitophagy; (2) MPTP toxicity seems to alter ROS generation rather than mitochondrial depolarization. The effects of mitochondrial toxins do not seem to be a one-way manner. The information is available for understanding the pathogenesis in PD. Here, we touched on the fringes of molecular mechanisms of PINK1-parkin-mediated mitophagy. Further research will elucidate how this quality control system applies to neurons.

Abbreviations

CCCP: Carbonyl cyanide m-chlorophenylhydrazone
DAT: Dopamine transporter
MEFs: Mouse embryonic fibroblasts
MPTP: 1-methyl-4-phynyl-tetrahydropyridine
PD: Parkinson's disease
PINK1: PTEN-induced putative kinase1
ROS: Reactive oxygen species
SN: Substantia nigra.

References

[1] G. C. Davis, A. C. Williams, S. P. Markey et al., "Chronic parkinsonism secondary to intravenous injection of meperidine analogues," *Psychiatry Research* , vol. 1, no. 3, pp. 249–254, 1979.

[2] J. W. Langston, P. Ballard, J. W. Tetrud, and I. Irwin, "Chronic parkinsonism in humans due to a product of meperidine-analog synthesis," *Science*, vol. 219, no. 4587, pp. 979–980, 1983.

[3] R. S. Burns, C. C. Chiueh, S. Markey, M. H. Ebert, D. Jakobowicz, and I. J. Kopin, "A primate model of Parkinson's disease, selective destruction of substantianigra, pars compactadopaminergic neurons by N-methyl-4-phenyl-1,2,3,6-tetrahydropyridine," *Proceedings of the National Academy of Sciences of the United States of America*, vol. 80, pp. 4546–4550, 1983.

[4] W. J. Nicklas, I. Vyas, and R. E. Heikkila, "Inhibition of NADH-linked oxidation in brain mitochondria by 1-methyl-4-phenyl-pyridine, a metabolite of the neurotoxin, 1-methyl-4-phenyl-1,2,5,6-tetrahydropyridine," *Life Sciences*, vol. 36, no. 26, pp. 2503–2508, 1985.

[5] R. R. Ramsay, J. I. Salach, J. Dadgar, and T. P. Singer, "Inhibition of mitochondrial NADH dehydrogenase by pyridine derivatives and its possible relation to experimental and idiopathic parkinsonism," *Biochemical and Biophysical Research Communications*, vol. 135, no. 1, pp. 269–275, 1986.

[6] Y. Mizuno, T. Saitoh, and N. Sone, "Inhibition of mitochondrial NADH-ubiquinone oxidoreductase activity by 1-methyl-4-phenylpyridinium ion," *Biochemical and Biophysical Research Communications*, vol. 143, no. 1, pp. 294–299, 1987.

[7] G. Fiskum, A. Starkov, B. M. Polster, and C. Chinopoulos, "Mitochondrial mechanisms of neural cell death and neuroprotective interventions in Parkinson's disease," *Annals of the New York Academy of Sciences*, vol. 991, pp. 111–119, 2003.

[8] D. T. Dexter, C. J. Carter, F. R. Wells et al., "Basal lipid peroxidation in substantia nigra is increased in Parkinson's disease," *Journal of Neurochemistry*, vol. 52, no. 2, pp. 381–389, 1989.

[9] E. Sofic, K. W. Lange, K. Jellinger, and P. Riederer, "Reduced and oxidized glutathione in the substantia nigra of patients with Parkinson's disease," *Neuroscience Letters*, vol. 142, no. 2, pp. 128–130, 1992.

[10] A. Yoritaka, N. Hattori, K. Uchida, M. Tanaka, E. R. Stadtman, and Y. Mizuno, "Immunohistochemical detection of 4-hydroxynonenal protein adducts in Parkinson disease," *Proceedings of the National Academy of Sciences of the United States of America*, vol. 93, no. 7, pp. 2696–2701, 1996.

[11] H. Shimura-Miura, N. Hattori, D. Kang, K. I. Miyako, Y. Nakabeppu, and Y. Mizuno, "Increased 8-oxo-dGTPase in the mitochondria of substantia nigral neurons in Parkinson's disease," *Annals of Neurology*, vol. 46, no. 6, pp. 920–924, 1999.

[12] Y. Mizuno, S. Ohta, M. Tanaka et al., "Deficiencies in complex I subunits of the respiratory chain in Parkinson 's disease," *Biochemical and Biophysical Research Communications*, vol. 163, pp. 1450–1455, 1989.

[13] A. H. V. Schapira, J. M. Cooper, D. Dexter, P. Jenner, J. B. Clark, and C. D. Marsden, "Mitochondrial complex I deficiency in Parkinson's disease," *The Lancet*, vol. 1, no. 8649, p. 1269, 1989.

[14] R. Betarbet, T. B. Sherer, G. MacKenzie, M. Garcia-Osuna, A. V. Panov, and J. T. Greenamyre, "Chronic systemic pesticide exposure reproduces features of Parkinson's disease," *Nature Neuroscience*, vol. 3, no. 12, pp. 1301–1306, 2000.

[15] M. H. Polymeropoulos, C. Lavedan, E. Leroy et al., "Mutation in the alpha-synuclein gene identified in families with Parkinson's disease," *Science*, vol. 276, no. 5321, pp. 2045–2047, 1997.

[16] R. Krüger, W. Kuhn, T. Müller et al., "Ala30Pro mutation in the gene encoding alpha-synuclein in Parkinson's disease," *Nature Genetics*, vol. 18, no. 2, pp. 106–108, 1998.

[17] J. J. Zarranz, J. Alegre, J. C. Gómez-Esteban et al., "The new mutation, E46K, of alpha-synuclein causes Parkinson and lewy body dementia," *Annals of Neurology*, vol. 55, no. 2, pp. 164–173, 2004.

[18] M. C. Chartier-Harlin, J. Kachergus, C. Roumier et al., "Alpha-synuclein locus duplication as a cause of familial Parkinson's disease," *The Lancet*, vol. 364, no. 9440, pp. 1167–1169, 2004.

[19] P. Ibáñez, A. M. Bonnet, B. Débarges et al., "Causal relation between alpha-synuclein gene duplication and familial Parkinson's disease," *The Lancet*, vol. 364, no. 9440, pp. 1169–1171, 2004.

[20] K. Nishioka, S. Hayashi, M. J. Farrer et al., "Clinical heterogeneity of alpha-synuclein gene duplication in Parkinson's disease," *Annals of Neurology*, vol. 59, no. 2, pp. 298–309, 2006.

[21] J. Fuchs, C. Nilsson, J. Kachergus et al., "Phenotypic variation in a large Swedish pedigree due to SNCA duplication and triplication," *Neurology*, vol. 68, no. 12, pp. 916–922, 2007.

[22] A. B. Singleton, M. Farrer, J. Johnston et al., "alpha-Synuclein locus triplication causes Parkinson 's disease," *Science*, vol. 302, no. 5646, p. 841, 2003.

[23] M. Farrer, J. Kachergus, L. Forno et al., "Comparison of kindreds with parkinsonism and alpha-synuclein genomic multiplications," *Annals of Neurology*, vol. 55, pp. 174–179, 2004.

[24] W. Dauer, N. Kholodilov, M. Vila et al., "Resistance of alpha-synuclein null mice to the parkinsonian neurotoxin MPTP," *Proceedings of the National Academy of Sciences of the United States of America*, vol. 99, no. 22, pp. 14524–14529, 2002.

[25] V. Bonifati, P. Rizzu, F. Squitieri et al., "DJ-1 (PARK7), a novel gene for autosomal recessive, early onset parkinsonism," *Neurological Sciences*, vol. 24, no. 3, pp. 159–160, 2003.

[26] R. M. Canet-Avilés, M. A. Wilson, D. W. Miller et al., "The Parkinson's disease DJ-1 is neuroprotective due to cysteine-sulfinic acid-driven mitochondrial localization," *Proceedings of the National Academy of Sciences of the United States of America*, vol. 101, no. 24, pp. 9103–9108, 2004.

[27] A. Mitsumoto and Y. Nakagawa, "DJ-1 is an indicator for endogenous reactive oxygen species elicited by endotoxin," *Free Radical Research*, vol. 35, no. 6, pp. 885–893, 2001.

[28] T. Taira, S. M. M. Iguchi-Ariga, and H. Ariga, "Co-localization with DJ-1 is essential for the androgen receptor to exert its transcription activity that has been impaired by androgen antagonists," *Biological and Pharmaceutical Bulletin*, vol. 27, no. 4, pp. 574–577, 2004.

[29] L. Zhang, M. Shimoji, B. Thomas et al., "Mitochondrial localization of the Parkinson's disease related protein DJ-1: implications for pathogenesis," *Human Molecular Genetics*, vol. 14, no. 14, pp. 2063–2073, 2005.

[30] E. Junn, W. H. Jang, X. Zhao, B. S. Jeong, and M. M. Mouradian, "Mitochondrial localization of DJ-1 leads to enhanced neuroprotection," *Journal of Neuroscience Research*, vol. 87, no. 1, pp. 123–129, 2009.

[31] R. H. Kim, P. D. Smith, H. Aleyasin et al., "Hypersensitivity of DJ-1-deficient mice to 1-methyl-4-phenyl-1,2,3,6- tetrahydropyrindine (MPTP) and oxidative stress," *Proceedings of the National Academy of Sciences of the United States of America*, vol. 102, no. 14, pp. 5215–5220, 2005.

[32] B. Thomas, R. von Coelln, A. S. Mandir et al., "MPTP and DSP-4 susceptibility of substantianigra and locus coeruleuscatecholaminergic neurons in mice is independent of parkin activity," *Neurobiology of Disease*, vol. 26, pp. 312–322, 2007.

[33] C. Wang, H. S. Ko, B. Thomas et al., "Stress-induced alterations in parkin solubility promote parkin aggregation and compromise parkin's protective function," *Human Molecular Genetics*, vol. 14, no. 24, pp. 3885–3897, 2005.

[34] N. Hattori, H. Matsumine, T. Kitada et al., "Molecular analysis of a novel ubiquitin-like protein (PARKIN) gene in Japanese families with AR-JP:, evidence of homozygous deletions in the PARKIN gene in affected individuals," *Annals of Neurology*, vol. 44, pp. 935–941, 1998.

[35] N. Abbas, C. B. Lücking, C. Ricard et al., "A wide variety of mutations in the parkin gene are responsible for autosomal

recessive parkinsonism in Europe," *Human Molecular Genetics*, vol. 8, pp. 567–574, 1999.

[36] M. Kann, H. Jacobs, K. Mohrmann et al., "Role of parkin mutations in 111 community-based patients with early onset parkinsonism," *Annals of Neurology*, vol. 51, pp. 621–625, 2002.

[37] N. L. Khan, E. Graham, P. Critchley et al., "Parkin disease: a phenotypic study of a large case series," *Brain*, vol. 126, no. 6, pp. 1279–1292, 2003.

[38] K. Hedrich, C. Eskelson, B. Wilmot et al., "Distribution, type and origin of Parkin mutations: review and case studies," *Movement Disorders*, vol. 19, no. 10, pp. 1146–1157, 2004.

[39] E. M. Valente, A. R. Bentivoglio, P. H. Dixon et al., "Localization of a novel locus for autosomal recessive early-onset parkinsonism, PARK6, on human chromosome 1p35-p36," *American Journal of Human Genetics*, vol. 68, no. 4, pp. 895–900, 2001.

[40] E. M. Valente, P. M. Abou-Sleiman, V. Caputo et al., "Hereditary early-onset Parkinson's disease caused by mutations in PINK1," *Science*, vol. 304, no. 5674, pp. 1158–1160, 2004.

[41] Y. Hatano, Y. Li, K. Sato et al., "Novel PINK1 mutations in early-onset parkinsonism," *Annals of Neurology*, vol. 56, no. 3, pp. 424–427, 2004.

[42] D. G. Healy, P. M. Abou-Sleiman, J. M. Gibson et al., "PINK1 (PARK6) associated Parkinson disease in Ireland," *Neurology*, vol. 63, no. 8, pp. 1486–1488, 2004.

[43] C. F. Rohé, P. Montagna, G. Breedveld, P. Cortelli, B. A. Oostra, and V. Bonifati, "Homozygous PINK1 C-terminus mutation causing early-onset parkinsonism," *Annals of Neurology*, vol. 56, no. 3, pp. 427–431, 2004.

[44] Y. Li, H. Tomiyama, K. Sato et al., "Clinicogenetic study of PINK1 mutations in autosomal recessive early-onset parkinsonism," *Neurology*, vol. 64, no. 11, pp. 1955–1957, 2005.

[45] J. W. Pridgeon, J. A. Olzmann, L. S. Chin, and L. Li, "PINK1 protects against oxidative stress by phosphorylating mitochondrial chaperone TRAP1," *PLoS Biology*, vol. 5, no. 7, article e173, 2007.

[46] N. Exner, B. Treske, D. Paquet et al., "Loss-of-function of human PINK1 results in mitochondrial pathology and can be rescued by parkin," *Journal of Neuroscience*, vol. 27, no. 45, pp. 12413–12418, 2007.

[47] M. E. Haque, K. J. Thomas, C. D'Souza et al., "Cytoplasmic Pink1 activity protects neurons from dopaminergic neurotoxin MPTP," *Proceedings of the National Academy of Sciences of the United States of America*, vol. 105, no. 5, pp. 1716–1721, 2008.

[48] A. Wood-Kaczmar, S. Gandhi, Z. Yao et al., "PINK1 is necessary for long term survival and mitochondrial function in human dopaminergic neurons," *PLoS ONE*, vol. 3, no. 6, Article ID e2455, 2008.

[49] J. C. Greene, A. J. Whitworth, I. Kuo, L. A. Andrews, M. B. Feany, and L. J. Pallanck, "Mitochondrial pathology and apoptotic muscle degeneration in Drosophila parkin mutants," *Proceedings of the National Academy of Sciences of the United States of America*, vol. 100, no. 7, pp. 4078–4083, 2003.

[50] J. Park, S. B. Lee, S. Lee et al., "Mitochondrial dysfunction in Drosophila PINK1 mutants is complemented by parkin," *Nature*, vol. 441, no. 7097, pp. 1157–1161, 2006.

[51] I. E. Clark, M. W. Dodson, C. Jiang et al., "Drosophila pink1 is required for mitochondrial function and interacts genetically with parkin," *Nature*, vol. 441, no. 7097, pp. 1162–1166, 2006.

[52] C. T. Chu, "Tickled PINK1: mitochondrial homeostasis and autophagy in recessive Parkinsonism," *Biochimica et Biophysica Acta*, vol. 1802, no. 1, pp. 20–28, 2010.

[53] S. Geisler, K. M. Holmström, D. Skujat et al., "PINK1/Parkin-mediated mitophagy is dependent on VDAC1 and p62/SQSTM1," *Nature Cell Biology*, vol. 12, no. 2, pp. 119–131, 2010.

[54] S. Kawajiri, S. Saiki, S. Sato et al., "PINK1 is recruited to mitochondria with parkin and associates with LC3 in mitophagy," *FEBS Letters*, vol. 584, no. 6, pp. 1073–1079, 2010.

[55] N. Matsuda, S. Sato, K. Shiba et al., "PINK1 stabilized by mitochondrial depolarization recruits Parkin to damaged mitochondria and activates latent Parkin for mitophagy," *Journal of Cell Biology*, vol. 189, no. 2, pp. 211–221, 2010.

[56] D. Narendra, A. Tanaka, D. F. Suen, and R. J. Youle, "Parkin is recruited selectively to impaired mitochondria and promotes their autophagy," *Journal of Cell Biology*, vol. 183, no. 5, pp. 795–803, 2008.

[57] D. P. Narendra, S. M. Jin, A. Tanaka et al., "PINK1 is selectively stabilized on impaired mitochondria to activate Parkin," *PLoS Biology*, vol. 8, no. 1, Article ID e1000298, 2010.

[58] C. Vives-Bauza, C. Zhou, Y. Huang et al., "PINK1-dependent recruitment of Parkin to mitochondria in mitophagy," *Proceedings of the National Academy of Sciences of the United States of America*, vol. 107, no. 1, pp. 378–383, 2010.

[59] A. Beilina, M. Van Der Brug, R. Ahmad et al., "Mutations in PTEN-induced putative kinase 1 associated with recessive parkinsonism have differential effects on protein stability," *Proceedings of the National Academy of Sciences of the United States of America*, vol. 102, no. 16, pp. 5703–5708, 2005.

[60] S. Takatori, G. Ito, and T. Iwatsubo, "Cytoplasmic localization and proteasomal degradation of N-terminally cleaved form of PINK1," *Neuroscience Letters*, vol. 430, no. 1, pp. 13–17, 2008.

[61] Y. Kim, J. Park, S. Kim et al., "PINK1 controls mitochondrial localization of Parkin through direct phosphorylation," *Biochemical and Biophysical Research Communications*, vol. 377, no. 3, pp. 975–980, 2008.

[62] C. Zhou, Y. Huang, Y. Shao et al., "The kinase domain of mitochondrial PINK1 faces the cytoplasm," *Proceedings of the National Academy of Sciences of the United States of America*, vol. 105, no. 33, pp. 12022–12027, 2008.

[63] C. H. Sim, D. S. S. Lio, S. S. Mok et al., "C-terminal truncation and Parkinson's disease-associated mutations down-regulate the protein serine/threonine kinase activity of PTEN-induced kinase-1," *Human Molecular Genetics*, vol. 15, no. 21, pp. 3251–3262, 2006.

[64] Y. Yang, Y. Ouyang, L. Yang et al., "Pink1 regulates mitochondrial dynamics through interaction with the fission/fusion machinery," *Proceedings of the National Academy of Sciences of the United States of America*, vol. 105, no. 19, pp. 7070–7075, 2008.

[65] C. A. Gautier, T. Kitada, and J. Shen, "Loss of PINK1 causes mitochondrial functional defects and increased sensitivity to oxidative stress," *Proceedings of the National Academy of Sciences of the United States of America*, vol. 105, no. 32, pp. 11364–11369, 2008.

[66] T. Amo, S. Sato, S. Saiki et al., "Mitochondrial membrane potential decrease caused by loss of PINK1 is not due to proton leak, but to respiratory chain defects," *Neurobiology of Disease*, vol. 41, no. 1, pp. 111–118, 2011.

[67] M. Shamoto-Nagai, W. Maruyama, Y. Kato et al., "An inhibitor of mitochondrial complex I, rotenone, inactivates proteasome

by oxidative modification and induces aggregation of oxidized proteins in SH-SY5Y cells," *Journal of Neuroscience Research*, vol. 74, no. 4, pp. 589–597, 2003.

[68] W. Dauer and S. Przedborski, "Parkinson's disease: mechanisms and models," *Neuron*, vol. 39, no. 6, pp. 889–909, 2003.

[69] V. Jackson-Lewis and S. Przedborski, "Protocol for the MPTP mouse model of Parkinson's disease," *Nature Protocols*, vol. 2, no. 1, pp. 141–151, 2007.

[70] J. Q. Trojanowski, "Rotenone neurotoxicity: a new window on environmental causes of Parkinson's disease and related brain amyloidoses," *Experimental Neurology*, vol. 179, no. 1, pp. 6–8, 2003.

Enhanced Hyperthermia Induced by MDMA in Parkin Knockout Mice

Y. Takamatsu[1], H. Shiotsuki[1,2], S. Kasai[1], S. Sato[2], T. Iwamura[3], N. Hattori[2] and K. Ikeda[1,*]

[1]*Division of Psychobiology, Tokyo Institute of Psychiatry, 2-1-8 Kamikitazawa, Setagaya-ku, Tokyo 156-8585, Japan;*
[2]*Department of Neurology, Juntendo University School of Medicine, 2-1-1 Hongo, Bunkyou-ku, Tokyo 113-8421, Japan;*
[3]*Matsuyama University College of Pharmaceutical Sciences, 4-2 Bunkyo-cho, Matsuyama, Ehime 790-8578, Japan*

Abstract: MDMA (3,4-methylenedioxymethamphetamine) is reportedly severely toxic to both dopamine (DA) and serotonin neurons. MDMA significantly reduces the number of DA neurons in the substantia nigra, but not in the nucleus accumbens, indicating that MDMA causes selective destruction of DA neurons in the nigrostriatal pathway, sparing the mesolimbic pathway. Parkinson's disease (PD) is a neurodegenerative disorder of multifactorial origin. The pathological hallmark of PD is the degeneration of DA neurons in the nigrostriatal pathway. Mutations in the parkin gene are frequently observed in autosomal recessive parkinsonism in humans. Parkin is hypothesized to protect against neurotoxic insult, and we attempted to clarify the role of parkin in MDMA-induced hyperthermia, one of the causal factors of neuronal damage, using parkin knockout mice. Body temperature was measured rectally before and 15, 30, 45, and 60 min after intraperitoneal injection of MDMA (30 mg/kg) at an ambient temperature of 22 ± 2°C. Significantly enhanced hyperthermia after MDMA injection was observed in heterozygous and homozygous parkin knockout mice compared with wildtype mice, suggesting that parkin plays a protective role in MDMA neurotoxicity.

Keywords: Hyperthermia, knockout, mice, MDMA, parkin.

INTRODUCTION

The amphetamine derivative 3,4-methylenedioxymethamphetamine (MDMA) is abused by young adults despite its potentially neurotoxic effects and psychiatric complications. MDMA produces a rapid enhancement of serotonin and dopamine (DA) release in the brain [1, 2]. Administration of MDMA in mice is well known to produce acute hyperthermia and degeneration of striatal DA nerve terminals [3]. Recently, Granado and colleagues [4] reported that MDMA produces a significant decrease in the number of tyrosine hydroxylase (TH)-immunoreactive neurons in the substantia nigra. This decrease was accompanied by a dose-dependent decrease in TH- and DA transporter (DAT)-immunoreactivity in the striatum. MDMA significantly reduces TH- and DAT-immunoreactivity in the striatum, but not in the nucleus accumbens, indicating that MDMA causes selective destruction of DA neurons in the nigrostriatal pathway, sparing the mesolimbic pathway. The degree of long-term neurodegeneration produced by MDMA appears to be closely related to the magnitude of the hyperthermic response [5]. Attenuation of the hyperthermia alleviates MDMA-induced loss of striatal dopamine [3].

Parkinson's disease (PD) is the most common neurodegenerative movement disorder. The major pathological hallmark of PD is the degeneration of DAergic neurons in the substantia nigra that innervate the striatum. The major symptoms of PD include tremor, bradykinesia, cogwheel rigidity, and postural instability, which arise from the degeneration of DAergic neurons in the substantia nigra. PD is a neurodegenerative disorder of multifactorial origin, and mutations in the gene encoding parkin, an E3 ubiquitin-protein ligase [6], are frequently observed in autosomal recessive parkinsonism in humans. The loss of parkin function has been suggested to result in aberrant accumulation of parkin substrate proteins [6]. Accumulation of these proteins has been postulated to confer toxicity to DAergic neurons in the substantia nigra [7].

In the present study, we hypothesized that parkin protects against neurotoxic insult, and we attempted to clarify the role of parkin in MDMA-induced hyperthermia, one of the causal factors of neuronal damage, using parkin knockout mice.

MATERIALS AND METHODS

Mice

Wildtype, heterozygous, and homozygous parkin knockout mice were prepared from heterozygous/heterozygous parkin knockout mouse crosses (21-37 g, 12-29 weeks of age). Mice were housed in an animal facility maintained at 22 ± 2°C and 55 ± 5% relative humidity under a 12/12 h light/dark cycle with lights on at 8:00 a.m. Food and water were available *ad libitum*. All behavioral testing was conducted during the light cycle. The experimental procedures and housing conditions were approved by the Institutional Animal Care and Use Committee of the Tokyo Institute of Psychiatry, and all animals were treated humanely in accordance with our institutional animal experimentation guidelines.

Body Temperature Measurement

Rectal temperature measurement was performed using a digital thermometer (BAT-12; Physitemp Instruments Inc.,

*Address correspondence to this author at the Division of Psychobiology, Tokyo Institute of Psychiatry, 2-1-8 Kamikitazawa, Setagaya-ku, Tokyo 156-8585, Japan; Tel: +81-3-3304-5701, ext; 508; Fax: +81-3-3329-8035; E-mail: ikeda-kz@igakuken.or.jp

1570-159X/11 $58.00+.00

Clifton, NJ, USA) with 0.1°C accuracy and a rectal probe for mice (RET-3, Physitemp Instrument Inc.). Each mouse was lightly restrained by hand for approximately 20 s while the probe was inserted approximately 2 cm into the rectum and a steady reading was obtained. Body temperature was measured rectally before and 15, 30, 45, and 60 min after intraperitoneal (i.p.) injection of MDMA (30 mg/kg) at an ambient temperature of 22 ± 2°C.

Drugs

MDMA was synthesized at Matsuyama University College of Pharmaceutical Sciences and freshly dissolved in saline. MDMA and vehicle were administered in a volume of 0.1 ml/10 g body weight.

Statistical Analysis

Mean and standard error were calculated from the values of 12-17 subjects. Changes in body temperature were analyzed by repeated-measures analysis of variance (ANOVA) followed by Scheffe's *post hoc* test. Baseline temperature and changes in body temperature areas-under-the-curve (AUC) were analyzed by one-way ANOVA and Scheffe's *post hoc* test.

RESULTS

Baseline Body Temperature in Parkin Knockout Mice

Baseline body temperature was measured before MDMA injection at room temperature (22 ± 2°C). No significant difference in baseline body temperature was observed among wildtype, heterozygous, and homozygous parkin knockout mice (Fig. **1**).

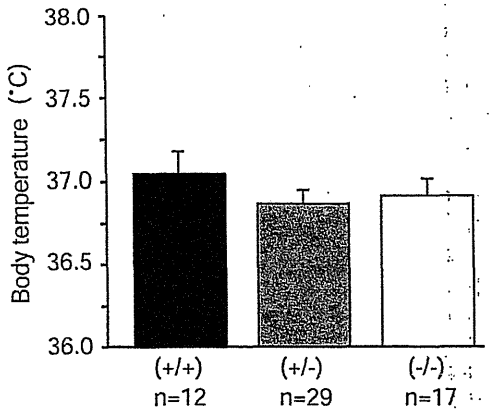

Fig. (1). No significant differences in baseline body temperature were observed among wildtype, heterozygous, and homozygous parkin knockout mice. Body temperature prior to MDMA injection did not significantly differ among genotypes. Baseline body temperature was analyzed by one-way ANOVA ($F_{2,55}$ = 0.629, p = 0.5369) at an ambient temperature of 22 ± 2°C.

No Sex Differences in MDMA-Induced Hyperthermia

Body temperature was measured 15, 30, 45, and 60 min after i.p. injection of MDMA (30 mg/kg) at an ambient temperature of 22 ± 2°C. No significant differences in MDMA-induced hyperthermia were observed between males and females within each genotype (Fig. **2**).

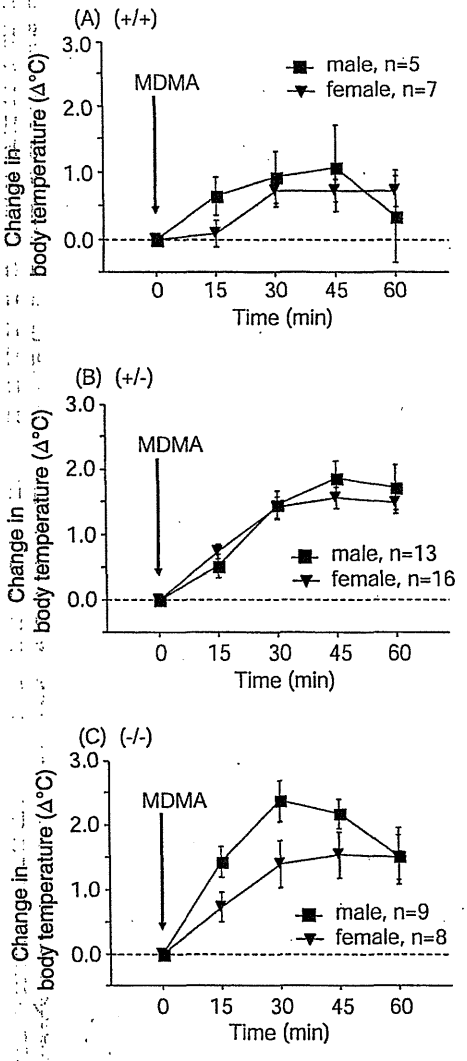

Fig. (2). Similar MDMA-induced (30 mg/kg, i.p.) hyperthermia was observed in male and female mice within each genotype. Body temperature areas-under-the-curve were analyzed by repeated-measures ANOVA. **(A)** Sex, $F_{1,10}$ = 0.181, p = 0.6796; Time, $F_{4,40}$ = 4.741, p = 0.0032; Sex × Time interaction, $F_{4,40}$ = 1.124, p = 0.3587. **(B)** Sex, $F_{1,27}$ = 0.134, p = 0.7170; Time, $F_{4,108}$ = 62.705, p < 0.0001; Sex × Time interaction, $F_{4,108}$ = 1.231, p = 0.3021. **(C)** Sex, $F_{1,15}$ = 2.350, p = 0.1461; Time, $F_{4,60}$ = 26.22, p < 0.0001; Sex × Time interaction, $F_{4,60}$ = 2.059, p = 0.0974.

Enhancement of MDMA-Induced Hyperthermia in Parkin Knockout and Heterozygous Mice

Body temperature gradually increased from baseline after MDMA injection in all genotype groups. MDMA significantly enhanced hyperthermia from 15 to 45 min after injection in parkin knockout mice and from 45 to 60 min after injection in heterozygous mice compared with wildtype mice (Fig. **3A**). MDMA produced hyperthermia, with a maximum increase of 0.9°C (37.9°C) 45 min after injection in wildtype mice, 1.7°C (38.6°C) 45 min after injection in heterozygous mice, and 1.9°C (38.8°C) 30 min after injection in parkin knockout mice. Body temperature AUC values reflected significantly enhanced hyperthermia in parkin knockout and heterozygous mice compared with wildtype mice (Fig. **3B**).

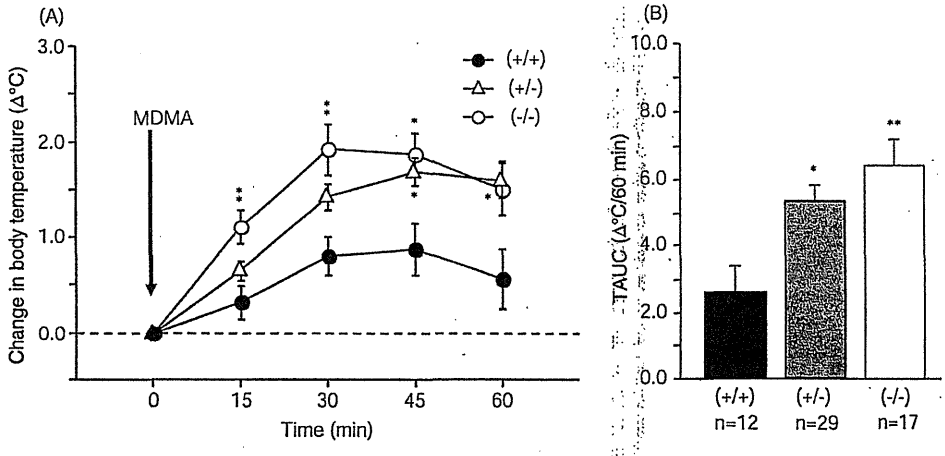

Fig. (3). Enhanced MDMA-induced hyperthermia in heterozygous and homozygous parkin knockout mice compared with wildtype mice. **(A)** Change in body temperature in mice injected with MDMA (30 mg/kg, i.p.). Body temperature areas-under-the-curve were analyzed by repeated-measures ANOVA (Genotype, $F_{2,55} = 6.746$, $p = 0.0024$; Time, $F_{4,220} = 61.267$, $p < 0.0001$; Genotype × Time interaction, $F_{8,220} = 3.664$, $p = 0.0005$) followed by Scheffe's *post hoc* test (*$p < 0.05$, **$p < 0.01$). **(B)** Change in body temperature areas-under-the-curve (TAUC) shown as an integration of the temperature *vs.* time curve shown in panel A. TAUC values were analyzed by one-way ANOVA ($F_{2,55} = 6.746$, $p = 0.0024$) followed by Scheffe's *post hoc* test (*$p < 0.05$, **$p < 0.01$).

DISCUSSION

In the present study, significantly enhanced MDMA-induced hyperthermia was observed in parkin knockout and heterozygous mice compared with wildtype mice (Fig. **3B**). The enhanced MDMA-induced hyperthermia in parkin knockout mice supports the hypothesis that parkin protects against MDMA-induced neurotoxic insult.

Hyperthermia is one of the major symptoms of acute MDMA-induced toxicity, which has been shown to be affected by body temperature [3]. MDMA produces a rapid enhancement of DA release in the striatum [1] and preoptic anterior hypothalamus [8]. MDMA-induced hyperthermia was blocked by a DA D_1 receptor antagonist [9]. Moreover, both the hyperthermia and augmented DA levels in the preoptic anterior hypothalamus after i.p. MDMA injection were significantly reduced by pretreatment with a D_1 antagonist [8]. Interestingly, Sato *et al.* (2006) [10] reported that D_1 receptor levels in the striatum in parkin knockout mice was higher than in wildtype mice, although no change in TH-positive substantia nigra neurons was found in parkin knockout mice, and no significant decrease in DAT levels was observed in the striatum. Therefore, the enhanced MDMA-induced hyperthermia observed in the present study may be attributable to increased levels of D_1 receptors in parkin knockout mice.

Sato *et al.* (2006) [10] also suggested that presynaptic neurons (i.e., DAergic neurons) are functionally impaired in parkin knockout mice. DA synthesis is significantly decreased and methamphetamine-induced DA release is reduced in parkin knockout mice. Considering that DAergic neurons in the substantia nigra are severely damaged in PD patients, the enhanced MDMA-induced hyperthermia in parkin knockout mice may be attributable to functional impairment of DAergic neurons, although the relationship between hyperthermia and DAergic neuron dysfunction remains to be elucidated.

Additionally, we found no significant difference in baseline body temperature among wildtype, heterozygous, and homozygous parkin knockout mice (Fig. **1**). These data suggest that parkin does not play a crucial role in the system that maintains basal body temperature.

In conclusion, MDMA-induced hyperthermia was enhanced in parkin knockout and heterozygous mice compared with wildtype mice. Parkin is hypothesized to be critical for protecting DAergic neurons from toxic insult, and the present results suggest that parkin plays a protective role against MDMA-induced DAergic neuron neurotoxicity.

ACKNOWLEDGEMENTS

We acknowledge Mr. Michael Arends for his assistance with editing the manuscript and Ms. Junko Hasegawa for her assistance with genotyping mice. This work was supported by a research grant (17025054) from the MEXT of Japan, by grants from the MHLW of Japan (H17-pharmaco-001, H19-iyaku-023, and 18A-3 and 19A-8 for Nervous and Mental Disorders), by a grant from the Smoking Research Foundation, and by a grant from the Mitsubishi Foundation for Social Welfare Activities.

ABBREVIATIONS

ANOVA	=	Analysis of variance
DA	=	Dopamine
DAT	=	Dopamine transporter
MDMA	=	3,4-methylenedioxymethamphetamine
PD	=	Parkinson's disease
TH	=	Tyrosine hydroxylase

REFERENCES

[1] Camarero, J.; Sanchez, V.; O'Shea, E.; Green, A.R.; Colado, M.I. Studies, using *in vivo* microdialysis, on the effect of the dopamine uptake inhibitor GBR 12909 on 3,4-methylenedioxymethamphetamine ("ecstasy")-induced dopamine release and free radical formation in the mouse striatum. *J. Neurochem.*, **2002**, *81*, 961-972.

[2] Doly, S.; Valjent, E.; Setola, V.; Callebert, J.; Hervé, D.; Launay, J.M.; Maroteaux, L. Serotonin 5-HT_{2B} receptors are required for

3,4-methylenedioxymethamphetamine-induced hyperlocomotion and 5-HT release *in vivo* and *in vitro*. *J. Neurosci.*, **2008**, *28*, 2933-2940.

[3] Colado, M.I.; Camarero, J.; Mechan, A.O.; Sanchez, V.; Esteban, B.; Elliott, J.M.; Green, A.R. A study of the mechanisms involved in the neurotoxic action of 3,4-methylenedioxymethamphetamine (MDMA, "ecstasy") on dopamine neurones in mouse brain. *Br. J. Pharmacol.*, **2001**, *134*, 1711-1723.

[4] Granado, N.; O'Shea, E.; Bove, J.; Vila, M.; Colado, M.I.; Moratalla, R. Persistent MDMA-induced dopaminergic neurotoxicity in the striatum and substantia nigra of mice. *J. Neurochem.*, **2008**, *107*, 1102-1112.

[5] Malberg, J.E.; Seiden, L.S. Small changes in ambient temperature cause large changes in 3,4-methylenedioxymethamphetamine (MDMA)-induced serotonin neurotoxicity and core body temperature in the rat. *J. Neurosci.*, **1998**, *18*, 5086-5094.

[6] Shimura, H.; Hattori, N.; Kubo, S.; Mizuno, Y.; Asakawa, S.; Minoshima, S.; Shimizu, N.; Iwai, K.; Chiba, T.; Tanaka, K.; Suzuki, T. Familial Parkinson disease gene product, parkin, is a ubiquitin-protein ligase. *Nat. Genet.*, **2000**, *25*, 302-305.

[7] Xu, J.; Kao, S.Y.; Lee, F.J.; Song, W.; Jin, L.W.; Yankner, B.A. Dopamine-dependent neurotoxicity of α-synuclein: a mechanism for selective neurodegeneration in Parkinson disease. *Nat. Med.*, **2002**, *8*, 600-606.

[8] Benamar, K.; Geller, E.B.; Adler, M.W. A new brain area affected by 3,4-methylenedioxymethamphetamine: a microdialysis-biotelemetry study. *Eur. J. Pharmacol.*, **2008**, *596*, 84-88.

[9] Mechan, A.O.; Esteban, B.; O'Shea, E.; Elliott, J.M.; Colado, M.I.; Green, A.R. The pharmacology of the acute hyperthermic response that follows administration of 3,4-methylenedioxymethamphetamine (MDMA, "ecstasy") to rats. *Br. J. Pharmacol.*, **2002**, *135*, 170-180.

[10] Sato, S.; Chiba, T.; Nishiyama, S.; Kakiuchi, T.; Tsukada, H.; Hatano, T.; Fukuda, T.; Yasoshima, Y.; Kai, N.; Kobayashi, K.; Mizuno, Y.; Tanaka, K.; Hattori, N. Decline of striatal dopamine release in parkin-deficient mice shown by *ex vivo* autoradiography. *J. Neurosci. Res.*, **2006**, *84*, 1350-1357.

Received: October 01, 2009 Revised: April 17, 2010 Accepted: May 26, 2010

Neurobiology of Disease 43 (2011) 651–662

Contents lists available at ScienceDirect

Neurobiology of Disease

journal homepage: www.elsevier.com/locate/ynbdi

DJ-1 associates with synaptic membranes

Yukiko Usami [a], Taku Hatano [a], Satoshi Imai [b,1], Shin-ichiro Kubo [a], Shigeto Sato [a], Shinji Saiki [a], Yoichiro Fujioka [c], Yusuke Ohba [c], Fumiaki Sato [b,2], Manabu Funayama [a,b], Hiroto Eguchi [a], Kaori Shiba [b], Hiroyoshi Ariga [d], Jie Shen [e], Nobutaka Hattori [a,b,*]

[a] Department of Neurology, Juntendo University School of Medicine, Japan
[b] Research Institute for Diseases of Old Age, Graduate School of Medicine, Juntendo University, Japan
[c] Laboratory of Pathophysiology and Signal Transduction, Hokkaido University Graduate School of Medicine, Japan
[d] Graduate School of Pharmaceutical Sciences, Hokkaido University, Japan
[e] Center for Neurologic Diseases, Brigham and Women's Hospital Program in Neuroscience, Harvard Medical School, USA

ARTICLE INFO

Article history:
Received 6 February 2011
Revised 30 April 2011
Accepted 20 May 2011
Available online 30 May 2011

Keywords:
DJ-1
Parkinson's disease
Localization
Synaptic vesicles
Synaptophysin
VAMP2
Rab3A

ABSTRACT

Parkinson's disease (PD) is a neurodegenerative disorder caused by loss of dopaminergic neurons. Although many reports have suggested that genetic factors are implicated in the pathogenesis of PD, molecular mechanisms underlying selective dopaminergic neuronal degeneration remain unknown. *DJ-1* is a causative gene for autosomal recessive form of *PARK7*-linked early-onset PD. A number of studies have demonstrated that exogenous DJ-1 localizes within mitochondria and the cytosol, and functions as a molecular chaperon, as a transcriptional regulator, and as a cell protective factor against oxidative stress. However, the precise subcellular localization and function of endogenous DJ-1 are not well known. The mechanisms by which mutations in DJ-1 contributes to neuronal degeneration also remain poorly understood. Here we show by immunocytochemistry that DJ-1 distributes to the cytosol and membranous structures in a punctate appearance in cultured cells and in primary neurons obtained from mouse brain. Interestingly, DJ-1 colocalizes with the Golgi apparatus proteins GM130 and the synaptic vesicle proteins such as synaptophysin and Rab3A. Förster resonance energy transfer analysis revealed that a small portion of DJ-1 interacts with synaptophysin in living cells. Although the wild-type DJ-1 protein directly associates with membranes without an intermediary protein, the pathogenic L166P mutation of DJ-1 exhibits less binding to synaptic vesicles. These results indicate that DJ-1 associates with membranous organelles including synaptic membranes to exhibit its normal function.

Introduction

Parkinson's disease (PD) is the second most common neurodegenerative disorder next to Alzheimer's disease and is characterized by motor symptoms as cardinal features such as resting tremor, rigidity, bradykinesia and postural instability. Pathological hallmarks of PD include marked cell loss of dopaminergic neurons in the substantia nigra pars compacta which causes dopamine depletion in the striatum and the presence of intracytoplasmic inclusions known as Lewy bodies in the remaining neurons (Fearnley and Lees, 1991). Although most of the PD cases are sporadic, approximately 5% of PD patients have clear familial etiology. Thus, the presence of monogenic forms of familial PD tells us that genetic factors contribute to the pathogenesis of PD. Indeed, heterozygous and homozygous mutations in one of the responsible genes have been reported in sporadic cases, suggesting that genetic factors are implicated in the pathogenesis of PD. Until now, 9 genes for familial PD have been reported, and these include *α-synuclein*, *parkin*, *UCH-L*, *PINK-1*, *DJ-1*, *LRRK2*, *ATP13A2*, *PLA2G6*, and *FBXO7* (Hatano et al., 2009).

Previous reports have suggested that DJ-1 functions as a molecular chaperon (Lee et al., 2003), a transcriptional regulator (Kim et al., 2005; Niki et al., 2003; Shinbo et al., 2005; Takahashi et al., 2001), and as a cell protective factor against oxidative stress (Canet-Aviles et al., 2004; Taira et al., 2004b; Yokota et al., 2003). The localization of DJ-1 has been shown to be in mitochondria, cytosol, nucleus, and microsomes (endoplasmic reticulum (ER) and Golgi) (Bonifati et al., 2003; Canet-Aviles et al., 2004; Miller et al., 2003; Taira et al., 2004a). However, most studies have been performed by exogenous DJ-1 using overexpression systems. On the other hand, endogenous DJ-1 is present in synaptic terminals, in both axons and dendrites, as well as

Abbreviations: PD, Parkinson's disease; FRET, Förster resonance energy transfer; WT, wild type; ER, endoplasmic reticulum; KO, knockout; RT, room temperature; PBS, phosphate-buffer saline; FBS, fetal bovine serum; BSA, bovine serum albumin; Tfn-R, transferrin receptor; IR, immunoreactivity; HB, homogenizing buffer.

* Corresponding author at: Department of Neurology, Juntendo University School of Medicine, 2-1-1 Hongo, Bunkyo-ku, Tokyo 113-8421, Japan. Fax: +81 3 5800 0547.
E-mail address: nhattori@juntendo.ac.jp (N. Hattori).
[1] Present affiliation: Department of Toxicology, School of Pharmacy and Pharmaceutical Sciences, Hoshi University, Japan.
[2] Present affiliation: Department of Clinical Chemistry, School of Pharmacy and Pharmaceutical Sciences, Hoshi University, Japan.

Available online on ScienceDirect (www.sciencedirect.com).

0969-9961/$ – see front matter © 2011 Elsevier Inc. All rights reserved.
doi:10.1016/j.nbd.2011.05.014

in mitochondria (Olzmann et al., 2007; Zhang et al., 2005). However, the precise function and dynamics of DJ-1 related to vesicular trafficking remain unclear: In the present study, we demonstrate the association of endogenous DJ-1 with membranous organelles and the molecular interaction of recombinant DJ-1 protein with membranes in cultured cells. In addition, we examine whether pathogenic mutations found in *PARK7*-linked early onset PD patients may be affected by binding activities of DJ-1.

Materials and methods

Antibodies and recombinant proteins

Mouse monoclonal antibody (M043-3, Clone 3E8) and rabbit polyclonal antibody (NB300-270) for DJ-1 were obtained from Medical & Biological Laboratories Co. (MBL, Nagoya, Japan) and Novus Biologicals, Inc. (Littleton, CO), respectively. Rabbit polyclonal antibodies to Rab3A (sc-308), Rab4A (sc-312), Rab5B (sc-598), and Tom20 (sc-11415) were purchased from Santa Cruz Biotechnology (Santa Cruz, CA), and Rab7B (R4779) was obtained from Sigma (St. Louis, MO). Mouse monoclonal antibodies to synaptophysin were purchased from Chemicon International, Inc. (MAB5258, Temecula, CA) (used for immunoblotting) and Progen Biotechnik (61012, Heidelberg, Germany) (used for immunocytochemistry). Synaptotagmin (610434) and NMDAR1 (556308) were obtained from BD Biosciences Pharmingen (San Diego, CA). Other primary antibodies were Rab3A (107111, Synaptic Systems, Gottingen, Germany), anti-human transferrin receptor (13-6800, Zymed Laboratories, South San Francisco, CA), Parkin (#4211) and Calnexin (#2679S) (Cell Signaling, Danvers, MA), VAMP2 (NB300-595, Novus Biologicals, Inc.), BIP2 (ab21685, Abcam, Cambridge, MA), Hsp70 (610608, BD Transduction Laboratories), Mito Tracker Red CMXRos (M-7512, Molecular Probes), and total OXPHOS rodent WB antibody cocktail (MS604; MitoSciences, Eugene, Oregon). Secondary antibodies conjugated to horseradish peroxidase were purchased from GE HealthCare Bio-Sciences (Piscataway, USA). From Invitrogen Molecular Probes, 488 and 546 conjugated secondary antibodies were purchased. The vectors encoding GST-tagged WT and mutants DJ-1 (M26I, A104T, D149A, and L166P) were kindly provided by Hiroyoshi Ariga (Laboratory of Pharmaceutical Science, Hokkaido University).

Experimental animals (DJ-1 KO mice)

The DJ-1 KO mice (F2) were a kind gift from The Laboratory of Pharmaceutical Science, Hokkaido University. The DJ-1 KO mice were generated at the Center for Neurologic Diseases, Brigham and Women's Hospital Program in Neuroscience, Harvard Medical School (Goldberg et al., 2005). F2 progeny were backcrossed for five generations to C57BL/6 mice, and heterozygotes were intercrossed to generate homozygous mice for the targeted *DJ-1* allele. For the experiments, C57BL/6J mice and DJ-1 KO mice were used at 7 to 9 weeks of age. All animal experiments were carried out in accordance with the Ethics Review Committee for Animal Experimentation of Juntendo University School of Medicine.

Cell culture and transfection

SH-SY5Y cells and HeLa cells were grown in Dulbecco's modified Eagle's medium (D-MEM, Sigma) with 10% fetal bovine serum (FBS; Sigma) and 1% penicillin–streptomycin (PS; Invitrogen). SH-SY5Y cell culture medium was supplemented with 1% non-essential amino acid, 1% sodium pyruvate, and 1% L-glutamate (Invitrogen). The cells were cultured at 37 °C and 5% CO_2. PC12 cells were grown in D-MEM with 5% FBS and 10% horse serum. Primary cortical neurons containing glia cells were prepared from E15.5 C57BL/6J mice and cultured for growth on Fisher-brand cover glass (Fisher Scientific, Pittsburgh, USA) in starting medium (F12 and Minimum Essential Medium with 10% FBS, 1% PS, and 0.001% insulin) for 3 days, and incubated sequentially for 5 days with 0.5 μM Ara-C (Sigma) in maintenance medium (F12 and Minimum Essential Medium with 5% calf serum, 5% horse serum, 1% PS, and 0.001% insulin). HeLa cells were transfected with expression vectors for FLAG-DJ-1 WT, M26I, A104T, D149A, or L166P by using FuGENE HD Transfection Reagent (Roche). After 24 h, immunocytochemistry was performed on the cells.

Immunocytochemistry

Cells were fixed for 10 min in 4% paraformaldehyde and 0.5% sucrose in phosphate-buffered saline (PBS). The cells were permeabilized with PBS containing 0.2% Triton X-100 (Sigma) for 5 min at RT. For blocking, 1× BlockAce (Yukijirushi Co., Osaka, Japan) was used for SH-SY5Y cells, and 10% FBS and 1% bovine serum albumin (BSA) in PBS (primary cortical neurons from mice) was used for primary cortical neurons for 30 min. Cells were incubated overnight with primary antibodies at 4 °C. The cells were washed 3 times with PBS and were incubated at RT for 1 h with secondary antibodies. After the cells were washed 3 times with PBS, the slides were mounted with Vectashield (Vector Laboratories, Burlingame, CA) and analyzed using a Leica confocal microscopy.

Preparation of synaptosome fractions from mouse brain

Synaptic vesicles were prepared as described previously (Hatano et al., 2007; Hell, 1998), with some modification. Briefly, whole brains from 3 mice (C57BL/6J) at 7 to 9 weeks of age were placed into 8 ml ice-cold synaptosomal homogenizing buffer (HB) (0.32 M sucrose, 4 mM HEPES–NaOH, pH 7.4 with EDTA-free protease inhibitor cocktail Complete Mini, EDTA free). The tissues were homogenized using a glass-Teflon homogenizer (10 up and down strokes, 830 rpm). The homogenized brain sample was centrifuged at 1000g for 10 min at 4 °C. After the supernatant (S1-1) was removed, the pellet was re-suspended in 5 ml HB and was homogenized and centrifuged at the same speed. The supernatant (S1-2) was removed, and the pellet was resuspended in 3 ml HB, and was homogenized and centrifuged in the same manner. The pellet was considered the P1 fraction, while the supernatant (mixed with S1-1, S1-2, and S1-3) was centrifuged at 12,000g for 15 min at 4 °C. The supernatant (S2) was removed and the pellet (P2) was resuspended with HB, and then centrifuged for 15 min at 13,000g at 4 °C. After removal of the supernatant (S2′), the pellet (P2′) was collected as the crude synaptosome fraction. P2′ was subsequently re-suspended with HB to a final volume of 1 ml. The P2′ fraction was suspended with 4 ml of ice cold water in the EDTA-free protease inhibitor cocktail. The samples were homogenized by 6 up and down strokes of the glass-Teflon homogenizer at 830 rpm and mixed with 39 μl 1 M HEPES, pH 7.4, then centrifuged for 20 min at 33,000g at 4 °C. The lysate pellet was considered the LP1 fraction, and the supernatant (LS1) was centrifuged for 2 h at 260,000g at 4 °C. After the supernatant (LS2) was removed, the pellet (LP2) was resuspended with 300 μl of HB. To loosen the pellet, samples were extruded consecutively through a 23-gauge and a 26-gauge hypodermic needle attached to a 1 ml syringe. The concentration of protein in each of the fractions was calculated using the BCA protein assay kit (Pierce, Rockford, IL). Finally, the same amounts of proteins from each fraction were analyzed by SDS–PAGE followed by immunoblotting.

Sucrose gradients of LS1 fraction from mouse brain

The LS1 fraction was layered on top of a linear sucrose density gradient ranging from 0.2 to 2.0 M sucrose dissolved in HEPES buffer (pH 7.4), and ultra-centrifuged at 465,000g for 13 h at 4 °C. Each of the fractions (0.5 ml) was collected from the top of the gradient, and equal volumes of each fraction were subjected to SDS–PAGE followed by immunoblotting.

Preparation of magnetic beads cross-linked with antibodies

For the following experiments of immunoisolation and immunoprecipitation, the DJ-1 polyclonal antibody and the synaptophysin antibody, and the normal rabbit IgG and the normal mouse IgG as control, were cross-linked to protein G-coated magnetic beads (Dynabeads Invitrogen). The beads were washed 3 times with citrate buffer, and then 50 μl of magnetic bead slurry was combined with 50 μg of each antibody by rotating for 1 h at RT. The antibody-bound beads were washed 3 times with 0.2 M sodium borate buffer (pH 9.0), and then resuspended in 0.2 M sodium borate buffer containing dimethyl pimelimidate (Pierce Biotechnology). After reacting by rotating the samples for 1 h at RT, the supernatants were removed and the Dynabead pellets were washed 3 times with 0.2 M triethanolamine buffer (pH 8.0). The washed beads were suspended with 0.2 M triethanolamine buffer containing 50 mM glycine, and were reacted for 2 h at RT. The supernatant was removed and the beads were washed 3 times with PBS, stored at 4 °C with PBS containing 0.05% Tween 20, and used within 1 week of the reactions.

Immunoisolation and immunoprecipitation of LS1 fraction containing synaptic vesicles from the mouse brain

Immunoisolation: beads cross-linked with DJ-1 antibody and synaptophysin antibody, or beads cross-linked with normal rabbit IgG and normal mouse IgG were washed 6 times with PBS and were blocked for 1 h at RT using PBS containing 10% BSA as nonspecific competitor, followed by washing in PBS 3 times. In addition, each of the 1 ml LS1 fraction samples were immunoisolated with 37.5 μl of the beads cross-linked with antibody for a total of 12 h at 4 °C after blocking non-specific sites by rotating with the beads with the cross-linked normal rabbit IgG, or normal mouse IgG for 1 h at 4 °C. The pellets and supernatants were subjected to SDS–PAGE followed by immunoblotting using antibodies against the indicated proteins.

Immunoprecipitation: beads cross-linked with the antibodies, the same as in the immunoisolation protocol, were blocked using PBS containing 10% BSA for 1 h at RT. LS1 fractions (900 μl) were dissolved in 100 μl of 10× RIPA buffer (final concentration: 140 mM KCl, 20 mM HEPES–KOH (pH 7.3), 2 mM EDTA, protease inhibitors, and 1% Triton X-100), and then the samples were blocked by rotating with normal IgG for 1 h at 4 °C. The supernatants were immunoprecipitated with 12.5 μl of each of the beads cross-linked with antibody overnight at 4 °C. The pellets and supernatants were subjected to SDS–PAGE followed by immunoblotting using antibodies against the indicated proteins.

Förster resonance energy transfer (FRET)

Synaptophysin-YFP and pCAGGS-CFP vector were a kind of gift from the Department of Cellular Neurobiology Graduate School of Medicine University of Tokyo. CFP–DJ-1 and CFP–VAMP2 were generated by fusing in frame to the DJ-1 N-terminal or VAMP2 N-terminal coding region in the pCAGGS-CFP vector. HeLa cells were transfected with expression vectors for CFP–DJ-1 or CFP–VAMP2, and synaptophysin-YFP using FuGene HD (Roche), according to the manufacturer's instruction. After 24 h, the cells were imaged with an IX70 inverted microscope (Olympus, Tokyo, Japan) equipped with BioPoint MAC5000 excitation and emission filter wheels (Ludl Electronic Products Ltd., Hawthorne, NY) and a Cool SNAP-HQ cooled CCD camera (Roper Scientific, Trenton, NJ). The filters used were purchased from Omega Optical Inc. (Brattleboro, VT): two excitation filters, XF1071 (440AF21) for CFP and Förster resonance energy transfer (FRET), and XF1068 (500AF25) for YFP; an XF2034 (455DRLP) dichroic mirror; two emission filters, XF3075 (480AF30) for CFP and XF3079 (535AF26) for FRET and YFP. Cells were illuminated with a 75 W xenon lamp through a 6% ND filter. Exposure times for 3×3 binning were 100 ms to obtain fluorescence images and 20 ms to obtain differential interference contrast image. MetaMorph software (Universal Imaging, West Chester, PA) was used to control the CCD camera and filter wheels, and also for the analysis of the cell image data.

Sensitized FRET measurement was performed using the method by Gordon et al.(1998). Briefly, fluorescence images for more than 20 cells were acquired sequentially through YFP, CFP, and FRET filter channels. The background was subtracted from raw images before FRET calculations. The fractions of the bleed-through of CFP and YFP fluorescence through the FRET channel were 0.502 and 0.385, respectively. Corrected FRET ($FRET_C$) was therefore calculated on a pixel-by-pixel basis for the entire image by using the equation: $FRET_C = FRET - 0.502 \times CFP - 0.385 \times YFP$, where FRET, YFP, and CFP correspond to background-subtracted images of cells co-expressing CFP and YFP. Calculated $FRET_C$ values are expressed as box and whisker plots, where the highest and lowest boundaries of the box represent the 25th and 75th percentiles, respectively, and whiskers above and below the box designate the 10th and 90th percentiles, respectively; the line within the box indicates the median value. $FRET_C$ images are also presented in the pseudocolor mode.

Alternatively, 293F cells (Invitrogen) were transfected with expression vectors for CFP–DJ-1 or CFP–VAMP2, and synaptophysin-YFP using 293fectin (Invitrogen) according to the manufacturer's recommendation. After 24 h, the cells were analyzed by a Flicyme-300 flow cytometer (Mitsui engineering and Shipment, Tokyo, Japan), which is equipped with a 445 nm semiconductor laser and is able to measure the fluorescence lifetime of CFP in the frequency domain at a single cell level. Data were acquired using the machine-bundled software, and exported to FlowJo flow cytometry analysis software (Tree Star, Inc., Ashland, OR). Using a gate tool, a population that expresses both CFP and YFP was selected, and FRET efficiency (E) of each cell was calculated by the following equation: $E = 1 - \tau_d'/\tau_d$, where, τ_d' and τ_d are donor (CFP) lifetimes in the presence and absence of the acceptor chromophore, respectively. E values of all analyzed cells were plotted in box and whisker plots.

Confocal laser scanning microscopy

Confocal images were obtained using an FV-10i confocal microscope (Olympus, Tokyo, Japan). Image data were exported to MetaMorph software and fluorescence intensities on lines of interest were gauged by the "Line Scan" function and plotted.

Cell fractionation

For cell fractionation studies, cultured cells (PC12) were washed with PBS, scraped off the culture plate in PBS, and centrifuged at 600g for 5 min. Cell pellets were resuspended in homogenization buffer (20 mM HEPES pH 7.2 and 0.25 M sucrose) in the presence of a cocktail of protease inhibitor (Complete Mini, EDTA-free), and sonicated at 4 °C (10 s, 3 times). The nuclei and unbroken cells were then pelleted by centrifugation at 1000g for 10 min at 4 °C. The supernatant was centrifuged at 100,000g for 1 h at 4 °C to separate the cytosolic and membrane fractions. To study the effects of salts and non-ionic detergent on the solubilization of DJ-1, the membrane fractions were incubated on ice for 30 min with homogenization buffer with 50, 150, and 1000 mM sodium chloride or 1% Triton X-100. After separation of the soluble and insoluble materials by centrifugation (100,000g, for 1 h, at 4 °C), equal volumes of each fraction were subjected to immunoblot with DJ-1, Parkin, and Tfn-R antibodies.

Proteinase K (PK) digestion of PC12 cell membrane fractions

Membrane fractions were isolated from PC12 cells and incubated with 0, 20, 40, 60, 80, and 120 μl of Proteinase K (PK)-agarose (Sigma) at 30 °C with rotation for 1 h. PK beads were removed from the

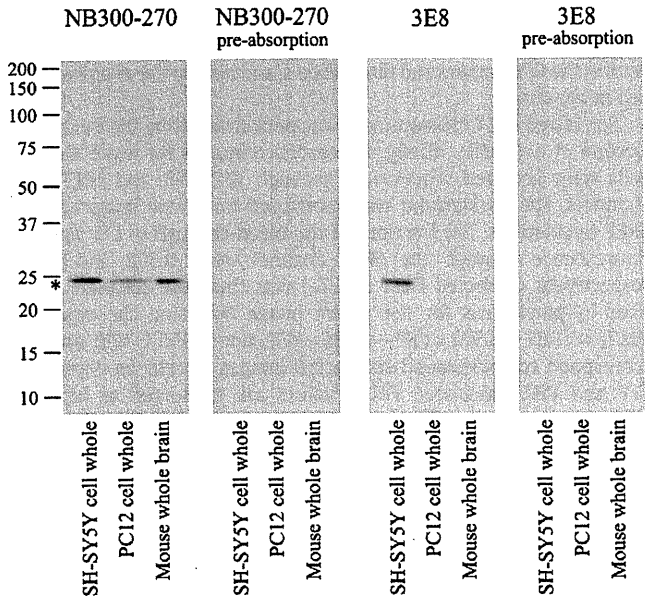

Fig. 1. Characterization of anti-DJ-1 antibodies. (A) Immunoblot of lysates from SH-SY5Y cells, PC12 cells, and mouse whole brain. Commercially available DJ-1 rabbit polyclonal antibody and mouse monoclonal antibody were used, as mentioned in Materials and methods. Specificities of these antibodies were confirmed by pre-absorption tests.

reacted membrane by centrifugation 5 times. PK-treated membranes were subjected to electrophoresis through Tris–HCl polyacrylamide gels (BIO-CRAFT) followed by staining with the GelCode SilverSNAP Stain Kit (Pierce).

In vitro binding assay by PC12 membranes

Recombinant DJ-1 WT, fused at its N terminus to the GST protein, or GST protein for negative control, were reacted with PC12 membranes, or PK-treated membranes (120 μl of PK beads concentration), at 30 °C for 1 h. The reacted samples were centrifuged at 100,000*g* for 1 h at 4 °C, and divided into supernatant and pellet. Both supernatant and pellet were subjected to SDS–PAGE followed by immunoblotting.

In vitro binding assay by LS1 fraction from DJ-1 KO mice

GST–DJ-1 WT recombinant protein (500 nM) or GST–DJ-1 mutant recombinant protein (M26I, A104T, D149A, and L166P) were combined with 200 μl of the LS1 fraction from DJ-1 KO mice ($n=3$), and rotated at 30 °C for 20 min. After treatment, the samples were centrifuged at 260,000*g* for 2 h at 4 °C. The supernatants were extracted and equal volumes of each fraction were subjected to immunoblot with anti-GST antibodies. The pellets were resuspended with the buffer (0.32 M sucrose-HEPES (pH 7.4) buffer) of equal volume, and equal volumes of each fraction were also subjected to immunoblot.

Immunoblotting

Cell lysates were mixed with LDS sample buffer (Invitrogen), heated for 5 min at 95 °C, and incubated on ice. The samples were resolved on 10–20% Tris–HCl gel (BIO CRAFT) in 1% SDS buffer and transferred onto polyvinylidene fluoride membranes (Bio-Rad Bioscience; Hercules, CA). The membranes were blocked for 1 h in TBS containing 0.1% Tween-20 (TBS-T) and 5% non-fat milk (BD Disco), and then incubated overnight at 4 °C with the primary antibody. The membranes were washed with TBS-T 3 times, followed by incubation for 1 h at RT with horseradish peroxidase-conjugated anti-mouse or anti-rabbit IgG. Immunoreactivity (IR) was assessed by a chemiluminescence reaction using Western Lightning (Perkin Elmer-Cetus, Foster City, CA) or ECL Plus reagent (GE Health Care Bio-Sciences).

Results

Characterization of anti-DJ-1 antibodies

To determine the endogenous localization of DJ-1, we employed the use of the commercially available mouse monoclonal and rabbit polyclonal DJ-1 antibodies. Immunoblot analyses using NB300-270 antibody (a rabbit polyclonal antibody) revealed a single band around 22 kDa corresponding to endogenous DJ-1 in the extracts from SH-SY5Y cells, PC12 cells, and mouse brain (Fig. 1). The 3E8 antibody, a mouse monoclonal antibody, also recognized a single band corresponding to the human DJ-1 protein in SH-SY5Y cells. However, this antibody did not detect the rodent DJ-1 protein in PC12 cells and mouse brain (Fig. 1). The band corresponding to DJ-1 disappeared when the antibody was pre-incubated with an excess amount of the antigen, confirming the specificity of the antibody (Fig. 1). Based on these results, the 3E8 antibody, which specifically recognizes endogenous human DJ-1, was used for immunocytochemistry, and the polyclonal NB300-270 antibody, which recognizes the mouse and rodent DJ-1 protein, was used for immunoblotting and immunocytochemistry of primary cortical neuronal cells obtained from mouse brain.

DJ-1 diffusely distributes with main membranous organelles

To examine the subcellular localization of DJ-1, SH-SY5Y cells were double-stained with the DJ-1 antibody and organelle-specific antibodies. Microscopic observation revealed diffuse DJ-1 immunostaining and the protein partly colocalized with GM130, a marker for Golgi apparatus. A small portion of DJ-1 colocalized with Mito Tracker and Tom20, both mitochondrial markers, and calnexin, an ER marker (Fig. 2A).

Based on the immunocytochemical data showing diffuse distribution of DJ-1 in cultured cells, we investigated the precise localization of DJ-1 using biochemical methods. To elucidate DJ-1 distribution in neuronal cells, mouse brain samples were fractionated by differential centrifugation and the fractions were analyzed for the presence of DJ-1 by immunoblotting (Fig. 2B). DJ-1 was present at considerable levels in the synaptosomes (P2′), which consisted of synaptic terminals including synaptic plasma membranes (LP1) and synaptic vesicles (LP2), and co-fractionated with synaptophysin, synaptotagmin, and

Fig. 2. DJ-1 was widely distributed with the main membranous organelles and synaptosomes. (A) SH-SY5Y cells were double-stained with antibodies to DJ-1 (green) and Mito Tracker, Tom20 (mitochondria), GM130 (Golgi apparatus), or calnexin (ER). Scale bars = 10 μm. (B) The experimental design of the synaptosome preparation is shown. (C) Subcellular fractionation of the mouse brain is described in Materials and methods. Aliquots of the subcellular fractions, containing 5 μg of protein, were analyzed by immunoblotting. NR-1 (membrane marker) was recognized in the LP1 fraction, and synaptophysin, synaptotagmin, and VAMP2 (vesicle marker) were detected in the LP2 fraction. Rab3A, Rab4A, Rab5B and Rab7B were widely concentrated in various subcellular fractions. DJ-1 was found in various fractions in conjunction with the Rab proteins. (D) Complex I–V (mitochondria), and GM130 (Golgi apparatus) organelle markers were investigated. Mitochondria were present in the P2′ and the LP1 fractions, but mitochondria were barely evident in the synaptic fraction. The Golgi fraction did appear in the cytosolic fraction (S2). (E) The amount of each fraction was quantified and graphed as a percentage for the estimated amount of whole brain protein. Data were the average ± SD of three independent experiments. (F) Using the results from panel C, immunoreactivity (IR) of each fraction was quantified and graphed as a percentage of each IR to the total immunoreactivities in DJ-1. Synaptophysin and NR-1 were compared with DJ-1 as well.

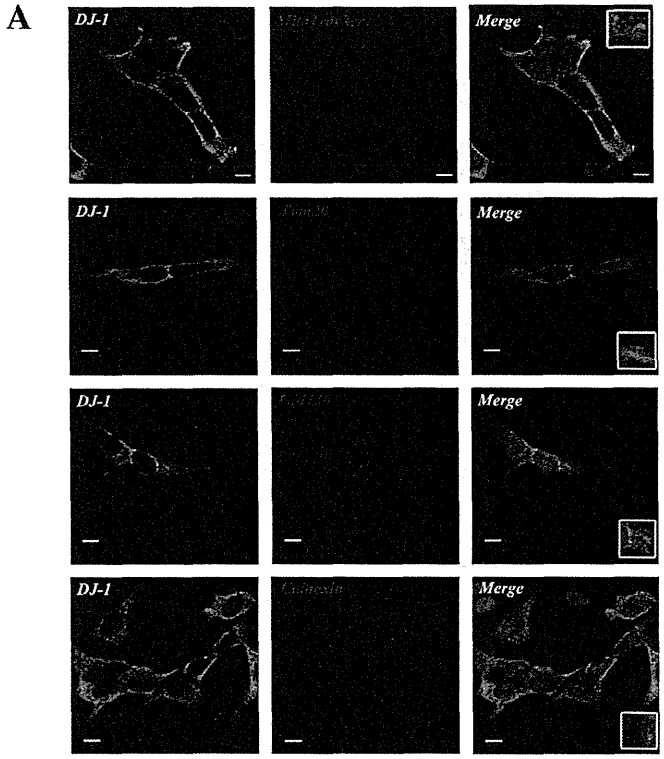
A
DJ-1
Merge
DJ-1
Merge
DJ-1
Merge
DJ-1
Merge

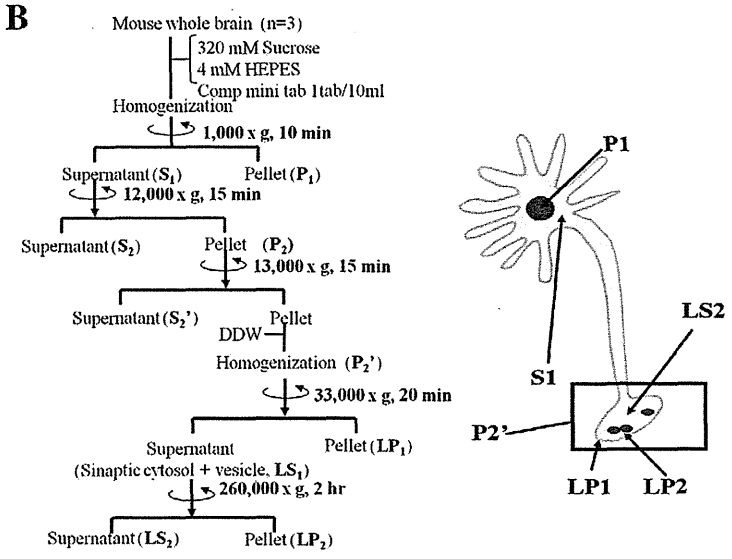
B
Mouse whole brain (n=3)
320 mM Sucrose
4 mM HEPES
Comp mini tab 1tab/10ml
Homogenization
1,000 x g, 10 min
Supernatant (S1)
Pellet (P1)
12,000 x g, 15 min
Supernatant (S2)
Pellet (P2)
13,000 x g, 15 min
Supernatant (S2')
Pellet
DDW
Homogenization (P2')
33,000 x g, 20 min
Supernatant
(Sinaptic cytosol + vesicle, LS1)
Pellet (LP1)
260,000 x g, 2 hr
Supernatant (LS2)
Pellet (LP2)
P1
S1
P2'
LS2
LP1
LP2

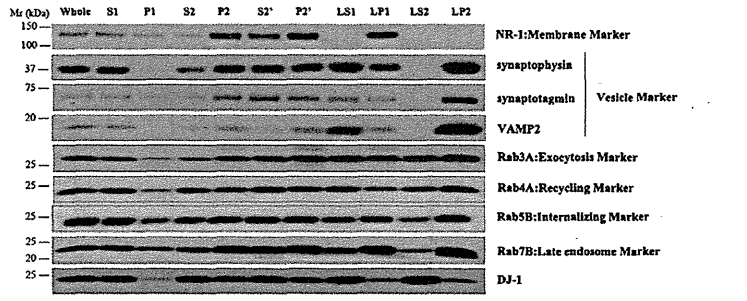
C
Mr (kDa)
Whole
S1
P1
S2
P2
S2'
P2'
LS1
LP1
LS2
LP2
150
100
37
75
20
25
NR-1:Membrane Marker
synaptophysin
synaptotagmin
Vesicle Marker
VAMP2
Rab3A:Exocytosis Marker
Rab4A:Recycling Marker
Rab5B:Internalizing Marker
Rab7B:Late endosome Marker
DJ-1

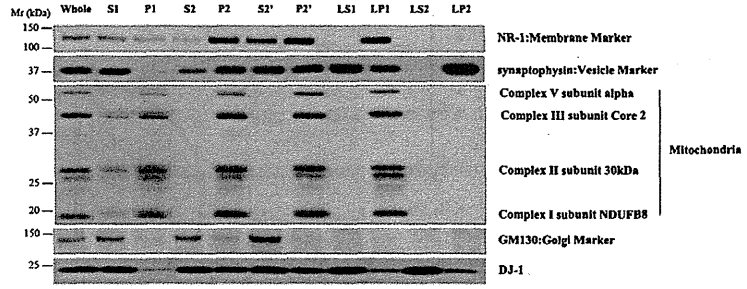
D
Mr (kDa)
Whole
S1
P1
S2
P2
S2'
P2'
LS1
LP1
LS2
LP2
150
100
37
50
25
20
NR-1:Membrane Marker
synaptophysin:Vesicle Marker
Complex V subunit alpha
Complex III subunit Core 2
Complex II subunit 30kDa
Complex I subunit NDUFB8
Mitochondria
GM130:Golgi Marker
DJ-1

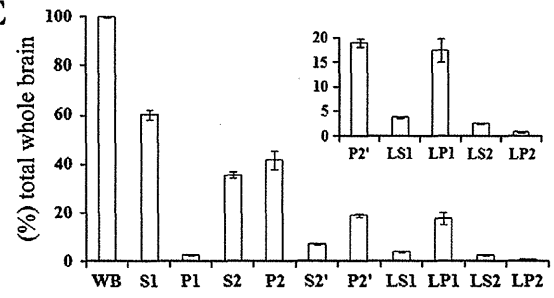
E
(%) total whole brain
100
80
60
40
20
0
WB
S1
P1
S2
P2
S2'
P2'
LS1
LP1
LS2
LP2
20
15
10
5
0

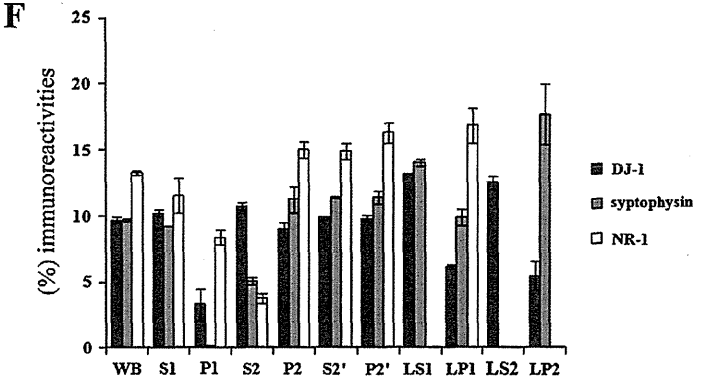
F
(%) immunoreactivities
25
20
15
10
5
0
WB
S1
P1
S2
P2
S2'
P2'
LS1
LP1
LS2
LP2
DJ-1
syptophysin
NR-1

VAMP2 (Fig. 2C). To further characterize the distribution of DJ-1 within synaptosomes, we investigated members of the family of monomeric GTPases called Rab proteins, such as Rab3A (exocytosis marker), Rab4A (recycling marker), Rab5B (endosome marker), and Rab7B (late endosome marker). As shown in Fig. 2B, these Rab proteins co-fractionated with DJ-1. However, mitochondrial respiratory complex proteins (Complex I subunit NDUFB8, Complex II subunit 30 kDa, Complex III subunit Core 2, and ATP synthase (Complex V) subunit α), which are mitochondrial markers, and the Golgi apparatus protein GM130, were not concentrated in the synaptic vesicle fraction (LP2) (Fig. 2D). The amount of each fraction was quantified and expressed as a percentage for the estimated amount of whole brain protein. The percentage of the P1 fraction was $2.69 \pm 0.20\%$, and DJ-1 was present in the nucleus, even though it was small. The percentages of P2′, LS1, LP1, LS2, and LP2, were $19.07 \pm 0.80\%$, $3.71 \pm 0.08\%$, $17.58 \pm 2.36\%$, $2.46 \pm 0.11\%$, and $0.75 \pm 0.19\%$, respectively (Fig. 2E). The amount of protein in the LP2 fraction was much less than that of the whole brain. DJ-1 IR of each fraction was quantified and shown as a percentage of each IR to total immunoreactivities. The percentage of DJ-1 IR of each fraction was $9.82 \pm 0.22\%$ (P2′), $13.19 \pm 0.07\%$ (LS1), $6.18 \pm 0.20\%$ (LP1), $12.54 \pm 0.50\%$ (LS2), and $5.43 \pm 1.08\%$ (LP2) (Fig. 2F).

DJ-1 localized on synaptic vesicles associated with synaptophysin and Rab3A

DJ-1 distributed with synaptic vesicles in the mouse brain (Fig. 2C). To elucidate the vesicle localization of DJ-1, the LS1 fraction containing synaptic vesicles and cytosol from mouse brain was further fractionated by sucrose density gradients centrifugation. Synaptophysin, VAMP2, synaptotagmin, and several Rab proteins were seen in fractions 9–18, and therefore, synaptic vesicles were collected in these fractions (Fig. 3A, B). Otherwise, the immunoreactivities of the synaptic vesicle markers were absent in fractions 1–8, suggesting that they were cytosolic fractions. The distribution of DJ-1 displayed biphasic peaks of both cytosolic fractions (fractions 1–8) and vesicle fractions (fractions 12–14). Coincidentally, the peak of DJ-1 IR agreed with the latter peak of synaptophysin and Rab3A (Fig. 3A, B). To further investigate the colocalization between DJ-1 and synaptic vesicles in neurons, primary cortical neuronal cells obtained from mouse brain were double-stained for DJ-1, and for synaptophysin or Rab3A. DJ-1 immunostaining appeared as punctate structures in the cytosol, axon, and synaptic terminals. DJ-1 was found to partly colocalize with synaptophysin and Rab3A, which play important roles in exocytosis (Edelmann et al., 1995; Handley et al., 2007) (Fig. 3C).

To gain further insight into the vesicle localization of DJ-1, immunoisolation was performed, as previously described (Burre et al., 2007; Morciano et al., 2005), with the LS1 fraction containing synaptic cytosol and vesicles from the mouse brain (Fig. 4A). To remove the nonspecifically interacting material, the LS1 fraction was treated with antibody-linked magnetic beads (Dyna-beads), which are cross-linked with normal rabbit or mouse IgG, and then the beads were removed. It was confirmed that DJ-1 and synaptophysin were not lost under this condition (Fig. 4B). Pre-cleaned LS1 was incubated with the Dyna-beads cross-linked with the DJ-1 antibodies, and then the vesicle isolates containing DJ-1 were subjected to immunoblotting with the DJ-1 antibody. Interestingly, synaptophysin and VAMP2 also localized with the DJ-1-associated vesicles (Fig. 4C). HSP70, which is known as a nuclear and cytosolic protein (Daugaard et al., 2007), was not isolated by this procedure (Fig. 4C). This indicates that the synaptic vesicle fraction was not contaminated with the cytosolic fraction. Therefore, this suggests that DJ-1, synaptophysin, and VAMP2 might localize on the surface of the same vesicle. In addition, it was further investigated whether DJ-1 directly interacts with synaptophysin and/or VAMP2. The LS1 fraction treated with RIPA buffer was immunoprecipitated with pull-down beads cross-linked

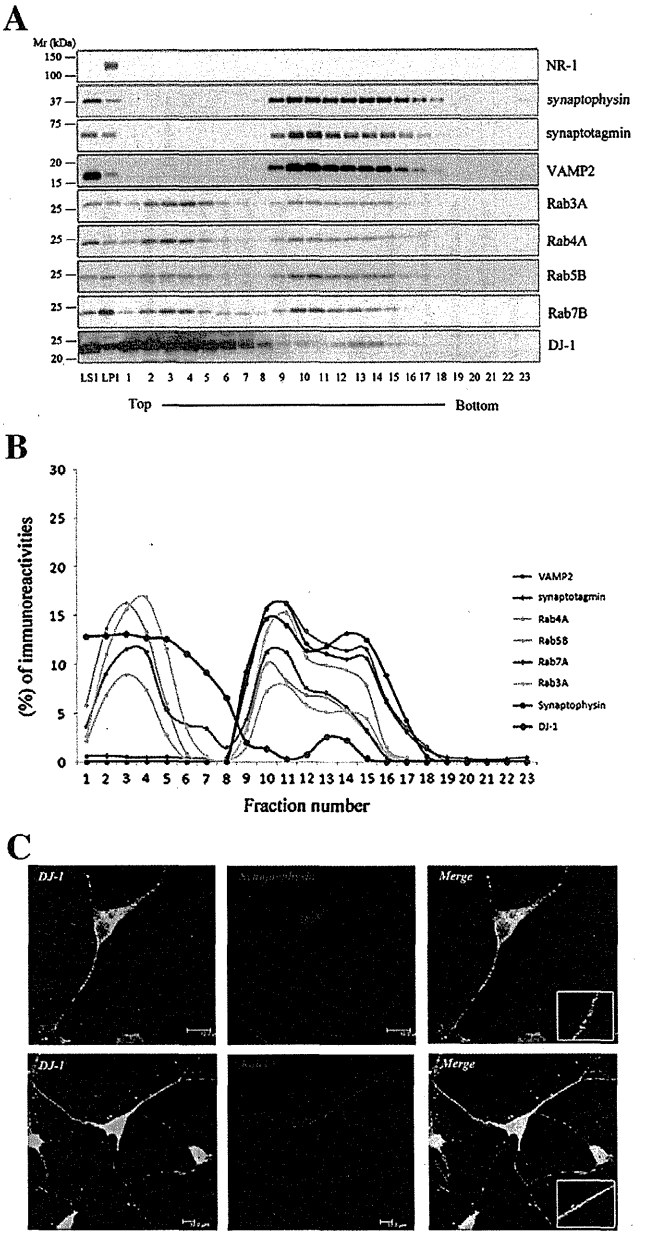

Fig. 3. DJ-1 associates with synaptic vesicles and colocalizes with synaptophysin and Rab3A. (A) The LS1 fraction was layered on top of a linear sucrose density gradient ranging from 0.2–2.0 M sucrose dissolved in HEPES buffer. Fractions were collected and 15 μl of each fraction were subjected to SDS–PAGE followed by immunoblotting using various markers. (B) Using the results from panel A, IR of each fraction was quantified and graphed as a percentage of each IR to the total immunoreactivities in each marker. DJ-1 had a biphasic profile of the immunoreactivities in fractions 1–8 and fractions 12–14, which indicated that there was some cytosolic fraction and some vesicle fractions. The peak of DJ-1 IR was in agreement with the latter peak of synaptophysin and Rab3A. (C) Primary cortical neurons from the mouse brain were fixed, permeabilized, and immunostained with DJ-1 antibody, and double-stained for synaptophysin and Rab3A. DJ-1 overlapped with synaptophysin and Rab3A. Scale bars = 10 μm.

with the synaptophysin antibody. It was found that VAMP2 interacts with synaptophysin as previous studies had reported (Baumert et al., 1989; Edelmann et al., 1995; Trimble et al., 1988). Immunoblotting with DJ-1 antibodies did not reveal endogenous DJ-1 in the resultant immunoprecipitates (Fig. 4C), whereas, endogenous synaptophysin and VAMP2 were not immunoprecipitated with the DJ-1 antibody.

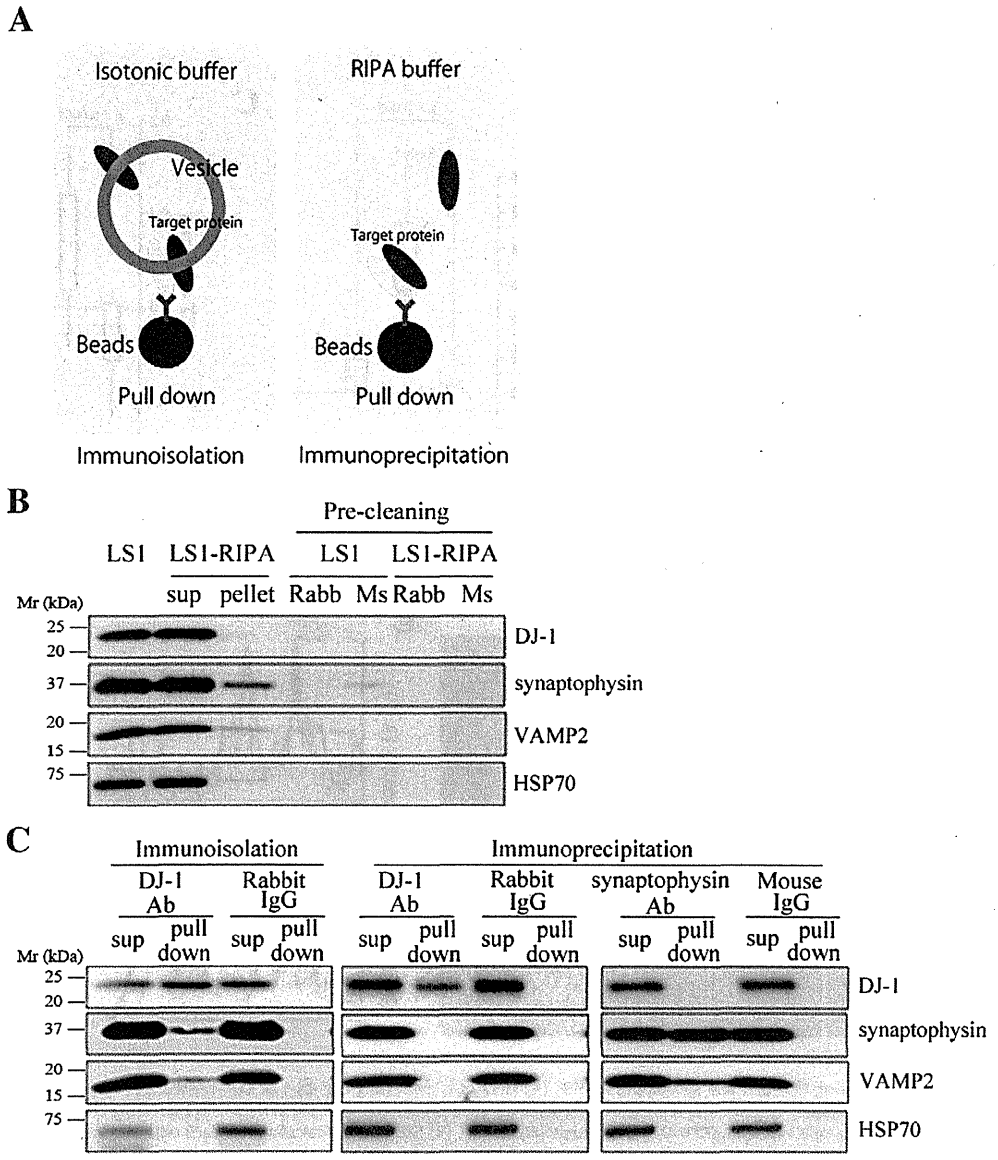

Fig. 4. DJ-1 cannot directly interact with synaptophysin and VAMP2, but associates with the same synaptic vesicles. (A) Image of immunoisolation and immunoprecipitation. Immunoisolation was used to pull down the target protein from the subcellular organelles (synaptic vesicle) from the homogenate, which was reacted with the isotonic buffer. Meanwhile, immunoprecipitation was used to pull down the target protein from the homogenate, which reacted with the buffer containing the detergent in order to examine the direct interactions between proteins. These methods were then used to assess the protein localized on the subcellular organelles with the target protein. (B) The LS1 fraction was first pre-cleaned. To remove nonspecifically-binding material, the LS1 fraction was treated with Dyna-beads cross-linked with normal rabbit or mouse IgG. It was confirmed that the targeting proteins were not lost in this reaction. (C) Sucrose buffer or RIPA buffer extracts of the mouse brain synaptic vesicle fractions were immunoisolated or immunoprecipitated using Dyna-beads coated with each antibody. Immunoisolates, immunoprecipitates and their corresponding supernatants were subjected to SDS–PAGE followed by immunoblotting using antibodies against the indicated proteins. Synaptophysin and VAMP2 were immunoisolated using Dyna-beads coated with the DJ-1 antibody, but they were not immunoprecipitated with the same bead slurry. Sup, supernatant.

Consequently, this proves that DJ-1 cannot directly interact with synaptophysin and VAMP2, but colocalizes with them on the same vesicles.

FRET analyses were performed to examine whether DJ-1 interacts with synaptophysin. We confirmed that FRET occurred between CFP–VAMP2, considered as positive control and synaptophysin-YFP (Pennuto et al., 2002). However, FRET was detected only in a small proportion of HeLa cells expressing CFP–DJ-1 and synaptophysin-YFP (Fig. 5A). $FRET_C$ median values with CFP–VAMP2, CFP–DJ-1, and CFP alone for more than 20 cells, were expressed as 0.363, 0.0413, and 0.0163, respectively (Fig. 5B). 293F cells expressing CFP–VAMP2 or CFP–DJ-1 and synaptophysin-YFP were also subjected to fluorescence lifetime flow cytometry, and fluorescence lifetimes of more than 10,000 cells in each sample were measured. Again, FRET efficiency observed between DJ-1 and synaptophysin was substantially lower than that between VAMP2 and synaptophysin, but significantly higher than that of the control (Fig. 5C). Confocal microscopic analyses revealed that CFP–DJ-1 also merged with synaptophysin-YFP. This pattern is similar to the colocalization between CFP–VAMP2 and synaptophysin-YFP (Fig. 5D, E). These results indicate that DJ-1 is able to localize with synaptophysin-positive vesicles and may interact with synaptophysin in living cells.